ISSN 0469-4732

INSTITUTE OF PLASMA PHYSICS

NAGOYA UNIVERSITY

IGNITION OF DEUTERIUM BASED FUEL CYCLES
IN A HIGH BETA SYSTEM

K. HIRANO

(Received – Dec. 22, 1986)

IPPJ-810 Jan. 1987

RESEARCH REPORT

NAGOYA, JAPAN

IGNITION OF DEUTERIUM BASED FUEL CYCLES IN A HIGH BETA SYSTEM

K. HIRANO

(Received – Dec. 22, 1986)

IPPJ-810 Jan. 1987

Institute of Plasma Physics, Nagoya University,

Nagoya, 464, Japan

ABSTRACT

A steady state self-consistent plasma modeling applied to a system having $<\beta>$ close to unity, such as FRC or like, is found to be quite effective in solving the problems independently of any anomalous process and proves the existence of ignited state of deuterium based fuel cycles. The temperature ranges that the plasma falls into ignited state are obtained as a function of relative feeding rates of tritium and ^3He to deuterium's. We find pure DD cycle will not ignite so that ^3He or/and tritium must be added as catalyzer to achieve ignition. Standing on the points to construct a cleaner system yielding smaller amount of 14 MeV neutrons and to burn the fuel in steady state for long periods of time, we have confirmed superiority of the complex composed of the master reactor of ^3He-$Cat.D$ cycle (catalyzed DD cycle reinjecting only fusion produced ^3He) and the satellite reactor of ^3He enriched D^3He cycle. In case storage of tritium for ^3He by β^- decay is turned out not to be allowed environmentally, we may utilize conventional catalyzed DD cycle although 14 MeV neutron yields will be increased by 35 % over the complex. It is demonstrated that advanced fuel cycle reactors can be very simple in constructions and compact in size such that the field strength and the plasma volume of the order of JT-60's may be enough for 1000 MW power plant.

1. INTRODUCTION

The final target of fusion study is in establishing a method and technics to construct a reactor to burn advanced fuels [1] , because deuterium is really inexhaustible resource and obtainable everywhere only if there is water. As a matter of fact, natural abundance of deuterium and the energy from the advanced fuel burn show a litter of water contains energy of 12 GJ. We know this quantity of energy is equivalent to that from about 320 litters of oil or 400 kg of coal. In spite of really attractive and challenging nature of the subject, advanced fuel has not been paid much attention to so far, because it requires the greater Lawson parameter by an order of magnitude and higher plasma temperature than *DT* does. In addition, we also learned that, if we wish to construct an advanced fuel reactor by usual low beta system such as tokamak or stellarator, severe cyclotron radiation loss due to required high temperature inhibits the ignition unless very high reflectivity of cyclotron radiation on the first wall is assumed [2] . We believe all the difficulties appearing in an advanced fuel reactor arise from the fact that we have not considered the ideal magnetic confinement system having $\langle\beta\rangle$ close to unity in detail so far.

Encouraged by recent success in FRC (Field Reversed Configuration), we endeavored to answer the question 'what is the ideal magnetic confinement system' in ref. [3] , and presented a scenario leading to catalyzed *DD* burn as an application of the study. This paper is written as a supplement to ref. [3] and describes the ignited states of deuterium based

fuel cycles in general under $\langle\beta\rangle\sim 1$ condition.

The most important point we have noticed so far in the study of $\langle\beta\rangle\sim 1$ toroidal system is in the fact that a plasma gains 'homeostasis' at $\langle\beta\rangle\sim 1$ state. For instance energy confinement time τ_E becomes independent of any transport mechanism in explicit manner but is determined by the total plasma heating power $\hat{W}_H$, external field strength B_{ex} and total plasma volume $\hat{V}_p$. These situations may be understood if we recall the definition of τ_E by

$$\tau_E = \frac{3}{2}\langle p\rangle\frac{\hat{V}_p}{\hat{W}_H} = \frac{3}{2}\langle\beta\rangle\frac{B_{ex}^2}{2\mu_0}\frac{\hat{V}_p}{\hat{W}_H} \quad . \tag{1-1}$$

The key issue giving the plasma homeostasis may be ascribed to the sharp pressure gradient or the thin field sheath necessary appearing on the surface of $\langle\beta\rangle\sim 1$ plasma. It may be suggested that, if $\hat{W}_H$, B_{ex} and $\hat{V}_p$ are given parameters, the thickness of the sheath layer is affected by transport properties; greater the anomalies larger becomes the sheath. We find in case enlarged sheath thickness by anomalies is still much smaller than the radius of the plasma eq.(1-1) shows τ_E is independent of anomalies since $\langle\beta\rangle\sim 1$ is not violated. As for an another example of homeostatic behavior of the plasma, we can refer the property that, if averaged density $\langle n\rangle$, B_{ex} and $\hat{V}_p$ are kept constant, averaged plasma temperature $\langle T\rangle$ will also keep a constant value even if we increase $\hat{W}_H$. Actually eq.(1-1) shows τ_E is inversely proportional to $\hat{W}_H$ so that increase of $\hat{W}_H$ will only lead enhanced transport loss. This indicates the thermal instability followed by fusion burn is stabilized at high $\langle\beta\rangle$

because temperature is unable to change independently. As a result, we may say heating up plasma to higher temperature requires simultaneous increase of $\hat{W}_H$ and B_{ex} if $\langle n \rangle$ and $\hat{V}_p$ are kept constant. Evidently, maintenance of the thin sheath on the plasma boundary for homeostasis requires steady high power input into the plasma. And we may have τ_E at ignited state without any detailed transport mechanism in case fusion burn delivers sufficiently high power to the plasma for keeping the sheath thin, which we believe true as is demonstrated in the subsequent sections and also partly in ref. [3] . Quantitative structures of homeostasis are presented in section 2. Owing to these peculiar property at high $\langle \beta \rangle$, we are able to solve the problem independently of transport model and clarify the ignition state with self consistent manner.

We would say that $\langle \beta \rangle \sim 1$ state not only gives plasma homeostasis but also is important in minimizing cyclotron loss [3] and the current driving power [3,4] into a level small enough as to give negligible effect on the global energy balance of the system. Moreover, the dangerous instabilities such as the tilting mode [5] , tearing mode [6] and n=2 rotational mode [7] have been demonstrated to be stabilized if $\langle \beta \rangle \sim 1$ is achieved. Because of so many advantages we believe detailed study of $\langle \beta \rangle \sim 1$ state in connection with fusion burn will play very important role in establishing the concept of the ideal advanced fuel cycle reactor.

In this paper we endeavored to answer the question 'what is the best fuel cycle'. The answer requires all the possible cycles capable of ignition. However, since Cordey [8]

demonstrated that the $p^{11}B$ cycle, the most probable cycle among 'exotic' fuel [1] , will not ignite because of too severe bremsstrahlung loss at high temperature, the study on deuterium based cycles consisting of DD, DT, and D^3He reactions may be enough for the answer.

This paper is written in the following order. The plasma modeling and the formal solutions are given in section 2, where we employ 1-D cylindrical model instead of the slab model in ref. [3] . In section 3, fusion burns are analysed for all the possible deuterium based fuel cycles using τ_E obtained in section 2, and attractive fuel cycles for power plant are proposed. Applicabilities and the limitations of the model are put into discussions in section 4, and in section 5 conclusions of the present study are presented.

2. STEADY STATE PLASMA MODELING AND THE SOLUTIONS

Since CT (Compact Torus) has much more advantages for reactor applications point of view than usual toroidal systems such as tokamak or stellarator, CT system or more specifically the simplest FRC has been considered as a representative of high beta toroidal systems in general. The same plasma model to the one of ref. [3] is also employed in this paper. We anticipate steady state plasma is maintained by beams and fusion burn; beams supply particles and the emf for current drive while the charged particle components of fusion products deliver heating power to keep the plasma temperature constant. We eventually

postulate that particle confinement time τ_p is much longer than the relaxation time τ_r of epithermal particles composed of injected beams and the fusion products so that the densities of thermal particles are assumed to be much greater than the ones of the epithermal particles. Then, as is discussed in detailed in ref. [3] , the moment equation sets derived from the Boltzmann equations for the thermal components of the distribution functions are simplified into the form tractable by analytic means under the four assumptions in the following.

(1) Stress tensors $\bar{\bar{\pi}}$ for all the particles species are neglected.

(2) All the temperatures for each species of particle are identical and homogeneous in the plasma.

(3) All the ion species have the same velocity in crossing the magnetic surfaces and in flowing along the field lines, which also claims electrons should take the same velocity to the ions' due to charge nuetrality.

(4) The emf to drive plasma current is generated by the bootstrap effect which carries the seed current induced by the flows of ions under the control of CBI (Counter Beam Injection) technics; gyrating beams of D^+ and $^3He^{++}$ in counter direction by each other with null net beam current are anticipated consequence of CBI [3,4] .

Owing to the assumptions of (1) and (4), we are able to use the global pressure balance equation,

$$\nabla p = \vec{j} \times \vec{B} \quad , \tag{2-1}$$

and the Ohm's law,

$$\vec{E} + \vec{v}_e \times \vec{B} + \frac{\nabla p_e}{e n_e} = \eta(\vec{j} - \vec{j}_*) \quad , \tag{2-2}$$

where η is the resisitivity and $\vec{j}_*$ is the current induced by the flow of ions. Using electron momentum balance and charge neutrality, we know $\vec{j}_*$ is given by

$$\vec{j}_* = \sum_\sigma (1 - \frac{Z_\sigma}{Z_{eff}})(\vec{j}_\sigma + \vec{j}_{\sigma x}) \quad , \tag{2-3}$$

where σ denotes ion species and the suffix σx the epithermal component σ species of ions, which is composed of the two parts: high energy beam component for heating and current drive, and low energy one for fueling. It is noted that assumption (4) or CBI claims the external control of the beam source to satisfy

$$\sum_\sigma \vec{j}_{\sigma x} = 0 \, . \tag{2-4}$$

Due to charge neutrality and assumption (3), the global particle balance may be described only by electron's, and we have

$$\nabla \cdot (n_e \vec{v}_e) = s_e^{(0)} \quad , \tag{2-5}$$

where $s_e^{(0)}$ denotes electron source density brought in by the relaxation of injected epithermal particles. From assumption (2), we also have energy conservation relation:

$$5 Z_p k T \nabla \cdot (n_e \vec{v}_e) = w_H \quad , \tag{2-6}$$

where w_H is the plasma heating power density and Z_p abbreviates $Z_p = (n_e + \sum_\sigma n_\sigma)/(2n_e)$. Here, we disintegrate w_H to write

$$w_H = s^{(2)} + w_{cF} - w_R \quad ,$$

where $s^{(2)}$ is the power imparted by externally injected beams, in which the power to drive the plasma current is included, w_{cF} the power due to charged particle components of fusion burn and w_R radiation loss. It is demonstrated in ref. [3] that, if fusion burn becomes important, $\langle\beta\rangle$ can be close to unity so that current driving power and cyclotron loss will be small enough to hold

$$w_H = w_{cF} - w_{brm} \quad , \tag{2-7}$$

where w_{brm} is bremsstrahlung loss. In order to have closed equation sets, we add

$$\mu_0 \vec{j} = \nabla \times \vec{B} \quad , \tag{2-8}$$

$$\nabla \times \vec{E} = 0 \quad , \tag{2-9}$$

$$p = 2Z_p k T n_e \quad , \tag{2-10}$$

and

$$n_e = \sum_\sigma Z_\sigma n_\sigma \quad . \tag{2-11}$$

In this paper we employ more realistic 1-D cylindrical model rather than the simpler slab model used in ref. [3] . A schematic drawing of a very elongated FRC for 1-D analysis is shown in Fig.1. After Hamada [9] we also postulate FRC is composed of the portion having straight field lines which are

ended by the short sections with curved field lines to connect between the inner and the outer volume separated by the field null surface at $r=R_0$. Let the length of the straight and the end section be L and L_{end}, respectively, then we require the separatrix radius R_s to satisfy $L \gg R_s$ and $L_{end} \sim R_s$, so that we may regard L be the total length of FRC. Here, we consider R_s may be given arbitrarily regardless of the wall radius, because axial equilibrium condition [10] can be adjusted by the mirror field at the end portion [11]. Since eq.(2-1) holds, the plasma pressure p and the field pressure B^2 on the same flux surface must be constant, so that p and B^2 at $r=r_{out}$ and $r=r_{in}$ should have the same value provided the two positions are related each other by

$$r_{out}^2 + r_{in}^2 = R_s^2 \quad . \tag{2-12}$$

This indicates that any pressure imbalance on the surface between and r_{out} and r_{in} is cured by the flow appearing along the field lines. In such a closed field configuration as depicted in Fig.1, it may be more convenient to introduce a new variable ξ defined by

$$\xi = (\frac{r}{R_0})^2 - 1 \quad . \tag{2-13}$$

Then, we know the interior of FRC is extended to the region $-1 \leqq \xi \leqq 1$. Using the variable ξ, we easily find eq.(2-12) can be rewritten as

$$\xi_{out} + \xi_{in} = 0 \quad , \tag{2-14}$$

so that we have parities

$$p(\xi) = p(-\xi) \ , \qquad n_e(\xi) = n_e(-\xi) \tag{2-15}$$

and

$$B(\xi) = -B(-\xi) \ . \tag{2-16}$$

Since the vector quantities $\vec{B}$, $\vec{j}$ and $\vec{j}_*$ have only one component B_z, j_θ and $j_{*\theta}$, respectively, in the present cylindrical coordinate system, it may be convenient and simpler to omit the suffixes to write B, j and j_*. Considering assumption (3) gives $v_{er}=v_r$ and $v_{ez}=v_z$, we have the following basic equation sets using variable ξ from eqs.(2-1),(2-2),(2-5),(2-8),(2-9) and (2-13):

$$(p + \frac{B^2}{2\mu_0})' = 0 \ , \tag{2-17}$$

$$\eta j_* = \eta j + B v_r \ , \tag{2-18}$$

$$\mu_0 j = -\frac{2}{R_0}(1 + \xi)^{1/2} B' \ , \tag{2-19}$$

and

$$\frac{2}{R_0}[n_e(1 + \xi)^{1/2} v_r]' + \frac{\partial}{\partial z}(n_e v_z) = s_e^{(0)} \ , \tag{2-20}$$

where the notation $(\ )'=d/d\xi$ has been introduced. The flow velocity v_z appearing in the LHS of eq.(2-20) is effective in eliminating inhomogeneity of density on the same flux surface.

In order to figure out v_z we postulate the odd parity:

$$v_z(\xi,z) = - v_z(-\xi,z) \ . \tag{2-21}$$

Then, writing eq.(2-20) at $\xi=\xi_1$ and $\xi=-\xi_1$ to be added and subtracted by each other, two relations are yielded by the parities:

$$\frac{2}{R_0}\left[n_e(1+\xi)^{1/2}v_r(\xi)\right]' - \frac{2}{R_0}\left[n_e(1-\xi)^{1/2}v_r(-\xi)\right]'$$

$$= s_e^{(0)}(\xi) + s_e^{(0)}(-\xi) \tag{2-22}$$

and

$$2n_e(\xi)\frac{\partial}{\partial z}v_z(\xi,z)+\frac{2}{R_0}\left[n_e(1+\xi)^{1/2}v_r(\xi)\right]'$$

$$+ \frac{2}{R_0}\left[n_e(1-\xi)^{1/2}v_r(-\xi)\right]' = s_e^{(0)}(\xi) - s_e^{(0)}(-\xi) \ , \tag{2-23}$$

where we omitted the suffix 1 for brevity. Equations (2-22) and (2-23) show that, if $s_e^{(0)}$ is independent of z, v_r becomes only a function ξ so that $v_z(\xi,z)$ must be proportional to z. Therefore, eq.(2-20) is reduced to be 1-D problem and we may have the same form to Hamada [9] :

$$v_z(\xi,z) = v_z(\xi,L/2)\cdot\frac{z}{L/2}.$$

where $v_z(\xi,L/2)$ is easily determined using eq.(2-23).

For convenience we introduce characteristic parameters; plasma radius $a(=R_s-R_0)$, the field diffusion time $\tau_d(=\mu_0 a^2/\eta)$

and characteristic electric field strength $E_d(=aB_{ex}/\tau_d)$ and $E_*(=\eta j_*)$ associated with field diffusion and current drive, respectively. Here, we dare to choose a as a characteristic scale length for τ_d anticipating easier comparison with the results of the slab model. As for the first step to solve the problem, we wish to find the field distribution in the plasma. Using eqs.(2-22), (2-18) and (2-19) we are able to have

$$b' - \left[\left(\frac{R_0}{2a}\right)^2 \frac{\tau_d}{n_e} \cdot \int_0^{\xi} s_{eA}^{(0)} d\xi\right] b = -\left(\frac{R_0}{2a}\right) \frac{E_*}{E_d} f(\xi) \quad , \tag{2-24}$$

where we utilize $b=B/B_{ex}$, $s_{eA}^{(0)}=\left[s_e^{(0)}(\xi)+s_e^{(0)}(-\xi)\right]/2$ and $f(\xi)=\left[(1+\xi)^{1/2}+(1-\xi)^{1/2}\right]/2$. In order to carry out integration of eq.(2-24) for b, we require information on $s_{eA}^{(0)}$. It is reminded that $s_e^{(0)}$ is written in the form,

$$s_e^{(0)}=n_e n_{ex} r_{rx} \quad ,$$

where suffix ex denotes the yet unrelaxed epithermal electron component and r_{rx} is the relaxation rate $\langle\sigma v_{rel}\rangle$ of n_{ex} into n_e. We assume for simplicity that particles and energies deposit only in the core region within $\pm\xi_c$ surface or the annular space between R_{ce} and R_{ci} in Fig.1. In addition, for the purpose of saving mathematical labors the distribution $n_{ex}r_{rx}$ in the core region is postulated to take

$$\sigma_e = \frac{n_{ex} r_{rx}}{n_{ex0} r_{rx0}} = 1 + \xi \frac{n_e'}{n_e} \quad , \tag{2-25}$$

where 0 appearing in the suffixes denotes the quantity on the surface of $r=R_0$. As is schematically shown in Fig.2, the label

to characterize the distribution of eq.(2-25) is chosen to be σ_{ec} or $\sigma_e(\xi_c)$. Evidently, inequality $0 \leqq \sigma_{ec} < 1$ holds since $\xi \cdot n_e'$ will never be positive. It is noted that the same sort of deposition and relaxation process is also assumed for all kinds of ion species. Here, we introduce a dimensionless quantity β_H defined by

$$\beta_H = \frac{2\mu_0}{B_{ex}^2} \frac{W_H \tau_d}{V_p}, \tag{2-26}$$

where we abbreviate $V_p = \pi R_s^2$ and

$$W_H = \int_{R_{c1}}^{R_{ce}} w_H \, 2\pi r dr = V_p \int_0^{\xi_c} w_H d\xi \quad .$$

Then, using eqs.(2-6),(2-17) and (2-25) with postulated boundary value $n_e(1)=0$ i.e. $b(1)=1$, which reflects the free expanding external plasma model gives $n_e(1)/n_e(0) \sim 10^{-4}$ [3], eq.(2-24) is modified to yield two separate equations for b:

1) the core region ($0 \leqq \xi \leqq \xi_c$)

$$b' - \frac{2}{5}\left(\frac{R_0}{2a}\right)^2 \beta_H \frac{\xi}{(1-b_c^2)\xi_c} b = -i \frac{f(\xi)}{\xi_c} \quad , \tag{2-27}$$

where $i = (R_0/2a) \cdot (E_*/E_d) \cdot \xi_c$, and

2) sheath region ($\xi_c \leqq \xi \leqq 1$)

$$b' - \frac{2}{5}\left(\frac{R_0}{2a}\right)^2 \beta_H \frac{b}{1-b^2} = 0 \quad . \tag{2-28}$$

As may be seen we find the slab model in ref.[3] can be easily converted into the cylindrical model if we multiply $(R_0/2a)^2$ or

the factor 1.457 to β_H, which indicates the cylindrical model gives better confinement than the slab.

Here, in order to solve the problem, β_H is treated as a given parameter under the postulated source distribution of the label σ_{ec}, and we wish to determine the three unknown parameters b_c, ξ_c and i appearing in eq.(2-27) and (2-28) as a function of β_H. We easily find the formal integration of eq.(2-27) gives

$$b(\xi_*) = -\, i\, exp(\beta_H^* \xi_*^2) \int_0^{\xi_*} f(\xi_c \cdot \xi_*) exp(-\beta_H^* \xi_*^2)\, d\xi_* \quad , \qquad (2\text{-}29)$$

where we utilize $\xi_*=\xi/\xi_c$ and

$$\beta_H^* = \frac{1}{5}\left(\frac{R_0}{2a}\right)^2 \frac{\xi_c}{1-b_c^2}\, \beta_H \quad .$$

Then, inserting $\xi_*=1$ into eq.(2-29), we have i of the form:

$$i = -\, b_c \frac{exp(-\beta_H^*)}{\int_0^1 f(\xi_c \cdot \xi_*) exp(-\beta_H^* \xi_*^2)\, d\xi_*} \quad . \qquad (2\text{-}30)$$

On the other hand, we have two more equations correlating among the three parameters. Integration of eq.(2-28) leads

$$\ln \frac{1}{b_c} - \frac{1}{2}(1-b_c^2) = \frac{2}{5}\left(\frac{R_0}{2a}\right)^2 \beta_H (1-\xi_c) \qquad (2\text{-}28)$$

while eqs.(2-25) and (2-27) at $\xi=\xi_c$ give

$$\sigma_{ec} = 1 - \frac{2 b_c \xi_c}{(1-b_c^2)} \left[\frac{2}{5}\left(\frac{R_0}{2a}\right)^2 \beta_H \frac{b_c}{1-b_c^2} - i \frac{f(\xi_c)}{\xi_c} \right] \quad . \qquad (2\text{-}32)$$

In case β_H is large enough to the extent

$$\beta_H \gg 0.55 \left| \left(ln \frac{1-\sigma_{ec}}{\beta_H} + 2.84 - 2\sigma_{ec} \right) \right| ,$$

which is satisfied for $\beta_H > 3$ provided σ_{ec} is not very close to unity, eqs.(2-30),(2-31) and (2-32) give approximate solutions:

$$b_c = 0.962 \left(\frac{1-\sigma_{ec}}{\beta_H} \right)^{1/2} \left[1 + \frac{0.429}{\beta_H} \left(\ln \frac{\beta_H}{1-\sigma_{ec}} - 2.84 + 2\sigma_{ec} \right) \right] \qquad (2\text{-}33)$$

and

$$\xi_c = 1 - \frac{0.858}{\beta_H} \left(\ln \frac{\beta_H}{1-\sigma_{ec}} - 0.847 \right) \qquad (2\text{-}34)$$

where we insert 1.21 into the factor $R_0/(2a)$. Using b_c and ξ_c thus obtained, we are able to have i from eq.(2-30), which means the problem is completely solved as a function of β_H.

In the first place we find the relation between $\langle\beta\rangle$ and the heating power W_H is expressed using β_H as

$$\langle\beta\rangle = 1 - \frac{0.429}{\beta_H} \left[1 - \frac{1.72(1-\sigma_{ec})}{\beta_H} \right] . \qquad (2\text{-}35)$$

Similarly, the sheath depth $d_{sh}^{(c)}$ from the surface to the core is found to be

$$d_{sh}^{(c)} = R_s - R_{ce} = 0.214 \frac{R_s}{\beta_H} \left(ln \frac{\beta_H}{1-\sigma_{ec}} - 1.22 \right) . \qquad (2\text{-}36)$$

It may be seen that the qualitative arguments about the plasma homeostasis in section 1 are justified with the quantitative background based on the binary collision model. Actually, eqs.(2-35) and (2-30) show that $\langle\beta\rangle\sim 1$ and $d_{sh}^{(c)} \ll R_s$ will be satisfied only if β_H is large enough. And in case plasma is in such a state perturbations on τ_d give only a small effect on $\langle\beta\rangle$ i.e. on τ_E, although $d_{sh}^{(c)}$ is affected to some extent. In section 4 some phenomenological discussions are given to show dependences of parameters on non ideal transport properties.

Here, we refer two important quantities: required total ion induced current $\hat{I}_*(=L\int_{R_{ci}}^{R_{ce}} j_* dr)$ for steady state and averaged number $\bar{s}$ of deuterium Larmor radii in a, which gives the criteria for the internal tilting mode being stabilized [5] . Assuming j_* is uniformly distributed in the core region, we have $\hat{I}_*$ if i is evaluated by eq.(2-30):

$$\hat{I}_* = \frac{2B_{ex}L}{\mu_0}\,\frac{(1+\xi_c)^{1/2}-(1-\xi_c)^{1/2}}{\xi_c}\cdot i \qquad (2\text{-}37)$$

On the other hand, eqs.(2-27) and (2-28) give rise to

$$\bar{s} = \int_{R_0}^{R_s}\frac{1}{R_s}\frac{r}{\rho_{iD}}dr = 7.09\times 10^{-10}\, Z_p^{1/2}\,\frac{N_{e0}^{1/2}}{\beta_H}\left(1-\frac{3}{2}b_c\right) , \qquad (2\text{-}38)$$

where ρ_{iD} is the Larmor radius of deuteron and electron line density $N_{e0}(=\pi R_s^2)$ is used.

Lastly, we point out that the most fundamental parameter β_H can only be determined after detailed scenario how we heat up the plasma. In this paper the heat source of the plasma is sought in fusion burns.

3. APPLICATION TO STEADY STATE IGNITED REACTOR

Utilizing the steady state solutions presented in previous section, we developed the analysis to clarify the condition that deuterium based fuel cycle are ignited. It is anticipated that the analysis reveals the most preferable fuel cycle. In subsection 3.1 the basic concept how we get solutions are described, and in following subsection 3.2 *DD* burns assisted by catalyzer are studied. Several examples showing the potentialities of advanced fuel cycle over *DT*'s are presented in subsection 3.3.

3.1 Basic Analysis Of Deuterium Based Fusion Burn

It is well known that deuterium based fusion reactions consist of the following four:

$$D + D \rightarrow {}^3He(0.82) + n(2.45) \qquad (DDn)$$

$$\rightarrow T(1.01) + p(3.02) \qquad (DDp)$$

$$D + {}^3He \rightarrow \alpha(3.66) + p(14.6) \qquad (D^3He)$$

$$D + T \rightarrow \alpha(3.52) + n(14.1)\ , \qquad (DT)$$

where numbers in parentheses are approximate energies of reaction products in MeV, and the nomenclatures of the reaction are indicated in the right parentheses. Here, we study the case

that all the plasma heating power is supplied by fusion burn and wish to estimate the value of w_{cF} in eq.(2-7) for β_H, since β_H gives any important parameter as indicated in the preceding section. In the first place, considering the result of preceding section, we assume $\beta_H>3$ for the purpose of successive approximation. Then, since the average value $<n_\sigma>$ of particle density of σ is defined by

$$<n_\sigma> = \frac{1}{\pi R_s^2}\int_0^{R_s} n_\sigma \, 2\pi r dr = \int_0^1 n_\sigma d\xi \quad ,$$

we find eq.(2-35) gives the inequality $1><\beta>\geqq 0.94$, and the approximation

$$<n_\sigma> = n_{\sigma 0}<\beta> \sim n_{\sigma 0} \tag{3-1}$$

is ensured. For the reason of brevity we omit the suffix 0 showing the quantity on the field null and simply write $n_\sigma=<n_\sigma>$ after eq.(3-1). Because of the assumption (3) in the preceding section, particle confinement time τ_p must be a common parameter for all the particle species and is defined by

$$\tau_p = \frac{\int_0^{R_s} n_e \, 2\pi r dr}{\int_{R_{c1}}^{R_{c2}} s_e^{(0)} \, 2\pi r dr} \quad . \tag{3-2}$$

Considering that $s_\sigma^{(0)}$ is composed of external particle injection rate g_σ and permutation rate due to fusion burn, we easily write down particle balance relations after eq.(2-5) taking care of eqs.(3-1) and (3-2):

$$g_D - \frac{1}{2}n_D^2 (r_{Dp} + r_{Dn}) - n_D n_3 r_{D3r}$$

$$- n_d n_T r_{DT} - \frac{n_D}{\tau_p} = 0 , \qquad (3\text{-}3)$$

$$g_T + \frac{1}{2}n_D^2 r_{Dp} - n_T n_D r_{DT} - \frac{n_T}{\tau_p} = 0 , \qquad (3\text{-}4)$$

$$g_3 + \frac{1}{2}n_D^2 r_{Dn} - n_D n_3 r_{D3} - \frac{n_3}{\tau_p} = 0 , \qquad (3\text{-}5)$$

$$\frac{1}{2}n_D^2 r_{Dp} + n_D n_3 r_{D3} - \frac{n_p}{\tau_p} = 0 , \qquad (3\text{-}6)$$

$$n_D n_3 r_{D3} + n_D n_T r_{DT} - \frac{n_\alpha}{\tau_p} = 0 , \qquad (3\text{-}7)$$

where g stands for averaged particle injection density $\langle g \rangle$, r the reactivity $\langle \sigma v \rangle$ of fusion burn, and following abbreviated suffixes are used: $^3He \rightarrow 3$, $DDn \rightarrow Dn$, $DDp \rightarrow Dp$ and $D^3He \rightarrow D3$. Equation (2-6) may be used to find out the relation $\tau_p = (5/3)\tau_E$. Then, the postulate of $\langle \beta \rangle \sim 1$ and eq.(1-1) yield

$$\tau_p = \frac{5}{2} \frac{p}{w_{cF} - w_{brm}} . \qquad (3\text{-}8)$$

Here, we may easily write down p and w_{cF} to give

$$p = kT(n_D + n_T + n_3 + n_p + n_\alpha + n_e) \qquad (3\text{-}9)$$

and

$$w_{cF} = \frac{1}{2}n_D^2 k \{ r_{Dn}E_3^{Dn} + r_{Dp}(E_T^{Dp} + E_p^{Dp}) \}$$

$$+ n_D n_3 r_{D3} k (E_\alpha^{D3} + E_p^{D3}) + n_D n_T r_{DT} k E_\alpha^{DT}, \qquad (3\text{-}10)$$

where E represents energy of fusion products in eV and the superscripts show the reaction concerned. Since at high temperature relativistic effect and e-e collision effect give important contribution to bremsstrahlung, the form given by Dawson [12] , which was a fit to numerical results of Maxson [13] , is applied:

$$w_{brm} = 1.49\times 10^{-38} Z_{eff} T^{1/2} n_e^2 (1+\frac{2T}{T_c})$$

$$\cdot \{1+\frac{2}{Z_{eff}} (1-\frac{1}{(1+T/T_c)^2}) \} \qquad (3\text{-}11)$$

where $T_c=m_e c^2/k$ is used.

Then, we notice that, if n_e is eliminated from eqs.(3-9) and (3-11) using eq.(2-11), the six equations from eq.(3-3) up to eq.(3-8) form a complete set giving restrictions among ten parameters: T, g_D, g_T, g_3, n_D, n_T, n_3, n_p, n_α and τ_p. In other word, we have four free parameters and remainder six are to be determined as a function of the given four. Considering deuterium is the basic fuel for every reactions, we believe the most convenient set of free parameters may be to choose T, n_D, α_T and α_3 where $\alpha_T=g_T/g_D$ and $\alpha_3=g_3/g_D$. Therefore, in DT case we set $\alpha_3=0$ while in D^3He burn we put $\alpha_T=0$.

The most eminent characteristics of the present model we have noticed in solving the problem is in the fact that the Lawson parameter $n_D\tau_E$ is independent of the density but determined by the temperature and the parameters α_T and α_3 representing the particular cycle we have chosen, because eq.(3-8) suggests τ_p is a function of the temperature and densities. In case we find the real roots under given four parameters, we may say the system is in ignited state, because plasma heating power is only supplied by charged particle components of fusion burn. In the first place we have studied the ignition temperature range for *DT* and D^3He burn. Results of the evaluated temperature ranges using the Maxwellian reaction rate by McNally et.al [14] are given in Fig.3 as a function of α_T and α_3. It is noted that, due to the particular property involved in the Lawson parameter, the temperature range is determined only by α_T and α_3. We can see that only in proper temperature range the plasma is ignited; at too low temperature fusion burn is insufficient while at too high temperature bremsstrahlung loss overwhelm the burn. We find in Fig.3 that pure *DD* burn ($\alpha_T=\alpha_3=0$) will not ignite, so that for *DD* burn we require catalyzer which can be ^3He or/and *T*. Detailed studies on *DD* burn using catalyzer are presented in the next subsection. In Fig.4 we give the Lawson parameters at ignited state as a function of temperature for five cases: 50-50 $DT(\alpha_T=1)$, 50-50 $D^3He(\alpha_3=1)$ and ^3He enriched $D^3He(\alpha_3=1.9)$, and also two different catalyzed burn, of which details are in the next subsection. We observe in Fig.4 that for a given temperature the Lawson parameter bifurcates and there appear two

roots. More generally, in case α_T and α_3 are given externally, only the value of the Lawson parameter on the bifurcated loops such as the ones in Fig.4 is allowed to exist at ignited state, or in other words, any deviation from the value on the curve is inhibited due to the tendency of the recurence to the original point.

One of the most important quantity we wish to know in addition to β_H is the total fusion power W_{Fus} per unit length of the system:

$$W_{Fus} = V_p \int_0^{\xi_c} (w_{cF} + w_{nF})\, d\xi \qquad (3\text{-}11)$$

where w_{nF} is the energy yield density of neutron components and is written by

$$w_{nF} = \frac{1}{2} n_D^2 r_{Dn} k E_n^{Dn} + n_D n_T r_{DT} k E_n^{DT} \ . \qquad (3\text{-}12)$$

It is noted in eq.(3-11) that for W_{Fus} we require the value of V_p or R_s in addition to the four parameters. We easily find W_{Fus} is written in the form

$$W_{Fus} = n_D^2 R_s^2 \, W(T,\ \alpha_T,\ \alpha_3),$$

so that the value of W_{Fus} is conveniently estimated in case we assign the reference values to n_D and R_s. And the values are chosen to be $n_D = 1 \times 10^{20}$ $(\mathrm{m})^{-3}$ and $R_s = 1$ m. Here, we put $\tilde{}$ on the quantity evaluated using the reference n_D and R_s, then we have

$$W_{Fus} = n_D^2 R_s^2 \tilde{W}_{Fus} \ , \qquad (3\text{-}13)$$

where n_{*D} is the density measured by the reference value of $\tilde{n}_D = 1\times10^{20}$ (m)$^{-3}$. As for β_H the relation becomes

$$\beta_H = n_{*D}R_s^2\tilde{\beta}_H \ . \qquad (3\text{-}14)$$

We may say in general that, if Q is some quantity which can be expressed as a function of the four parameters and R_s, then we are able to have proportionality between Q and $\tilde{Q}$. In order to show how $\tilde{Q}$ moves as a function of T, we typically take out $\tilde{W}_{Fus}$, $\tilde{W}_{nF}$, $\tilde{\beta}_H$, $\tilde{I}_D$, $\tilde{B}_{ex}$ and f_B where $\tilde{I}_D$ is the deuterium injection rate in current equivalent ($I_D=eV_pg_D$) and f_B is the burn fraction defined by $f_B=(I_D-I_{Dtr})/I_D$ where I_{Dtr} is the current equivalent of transport loss of deuterium. In Fig.5, we presented the case for 50-50 *DT* burn and highly ^3He enriched D^3He (α_T=0, α_3=1.9) burn giving the smallest neutron fraction to the fusion energy yield.

We can see in Figs.5-c and -f that the postulate β_H>3 for making $\langle\beta\rangle\sim1$ is safely satisfied at the reference parameter. Therefore, eq.(3-14) shows the postulate is always fulfilled unless we choose too small values of n_D and R_s. As in the case of the Lawson parameter, we find the solutions always bifurcate at the critical temperature into two states: low burn state (state-1) of smaller f_B and higher burn state (state-2) with greater f_B (see Fig.5-b and -c). Comparing the quantities in the state-1 with those in the state-2 in Fig.5, we easily notice $\tilde{W}_{Fus1}<\tilde{W}_{Fus2}$, $\tilde{W}_{nF1}<\tilde{W}_{nF2}$, $\tilde{I}_{D1}>\tilde{I}_{D2}$, $\tilde{B}_{ex1}<\tilde{B}_{ex2}$ and $\tilde{\beta}_{H1}>\tilde{\beta}_{H2}$. Evidently, all these effects are caused by the fact that high burn state accumulates larger portion of the ashes (α and p) in the plasma. In an economical point of view we consider the

choice of low burn state is preferable provided larger fuel supply is possible rather easily.

3.2 DD Burn With Catalyzer

Because neutrons produced by fusion burns in the reactor give structual material unfavorable radiation damages which not only spoil the strength of the material but also induce after heating effects, smallness of neutron fraction in fusion power, especially of 14 MeV component, is a very important item in constructing a cleaner fusion power plant. In this sense, ^3He enriched D^3He cycle may be the best one. However, the most decisive defect of D^3He cycle is in the scarcity of ^3He resources on this planet, although Wittenberg et al. [15] predict ^3He on the lunar surface can be extractable by commercial rate for the reactor. In spite of the superiority of D^3He cycle, we believe the study on efficient use of inexhaustible and easily extractable [16] terrestrial deuterium resources is of worth to work out.

Figure 3 shows that for DD cycle be ignited ^3He or T catalyzer is necessary. The easiest way to obtain the catalyzer is to reinject the convected out fusion products. Then, since the reinjection makes the cycle to close, we only have to supply deuterium. In order to pursue DD burn in very general way we propose the system shown in Fig.6, which consists of the master reactor and the ^3He enriched D^3He satellite supplemented with tritium reservoir for β^- decay into ^3He. The basic concept under the system in Fig.6 lies in the fact that we wish to reduce the high energy 14 MeV neutron component emitted from DT

reaction, because that component gives particularly unfavorable effects to structual materials: spoiling the strength and induction of after heating . Since the scarcity of 14 MeV neutron component can be an important measure of a cleaner reactor, we introduce parameters f_{nH} and γ which are

f_{nH} = numbers of 14 MeV neutron per GJ energy yield,

γ = relative numbers of 14 MeV neutrons to 50-50 DT's .

Evidently, f_{nH} and γ are the function of temperature and the cycle under consideration. We find 50-50 *DT* burn gives almost temperature independent value of $f_{nH}^{DT}=3.55\times10^{20}$ neutrons /GJ and D^3He burn of $\alpha_3=1.9$ takes fairly flat distribution having minimum value of $f_{nH}^{D3}=4.34\times10^{18}$ at T=91 keV, so that γ_{D3} becomes 1.22 %.

Although open and closure operation of the six valves in Fig.6 yields various catalyzed *DD* cycles, we have only considered the ones expected to give smaller γ and chosen three of them indicated in Table 1; Cat.D, ^3He-Cat.D, and ^3He-Cat.D-G (Gross), where Cat.D is usual catalyzed *DD* cycle reinjecting all the unburnt T and ^3He produced by *DD* reactions, ^3He-Cat.D is the cycle reinjecting only ^3He and T is stored in the reservoir for permutation into ^3He in order to use as a fuel of the satellite, and ^3He-Cat.D-G is catalyzed by all the ^3He including the one in the reservoir. It is noted that ^3He-Cat.D is operated to form the complex with the satellite reactor of ^3He enriched D^3He cycle of $\alpha_3=1.9$.

Analyses of each three catalyzed cycle become possible if the source terms g_T and g_3 are related with the flows of the fusion produced T and ^3He in the following way:

(1) $Cat.D$, $\quad g_T = \frac{n_T}{\tau_p}, \quad g_3 = \frac{n_3}{\tau_p}$

(2) ^3He-$Cat.D$ $\quad g_T = 0, \quad g_3 = \frac{n_3}{\tau_p},$

(3) ^3He-$Cat.D$-G $\quad g_T = 0, \quad g_3 = \frac{n_3}{\tau_p} + \varphi_{T3}\frac{n_T}{\tau_p}$,

where φ_{T3} is the fraction of n_T which is converted into ^3He in the reservoir. Since n_T/τ_p is a slowly varying function of time t in case the master reactor is operated in steady state for a long periods of time, φ_{T3} may be approximated as

$$\varphi_{T3} = 1 - exp(-\frac{t}{\tau_\beta}) \quad , \qquad (3\text{-}15)$$

where τ_β is the time constant of β^- decay and has the value of 17.7 years.

Consequently, we are able to solve the problem and find that the ignition temperature range of Cat.D and ^3He-Cat.D cycle is 38.1~113 keV and 38.3~115 keV, respectively, as is observed in Fig.4. We also evaluated the range of ^3He-Cat.D-G cycle to take 37.6~125 keV in case it is continuously operated for 30 years long. And we may say that the ranges for three catalyzed burns do not differ significantly, which simply comes from the fact that the range is exclusively a function of the amount of

^3He reinjected.

Because the satellite D^3He cycle is closely linked to the main ^3He-Cat.D reactor, we find the fusion out put power of the satellite is given by

$$W_{Fus}^{(S)} = 0.144\ \varphi_{T3} W_{Fus}^{(M)} \quad . \tag{3-16}$$

We also have f_{nH} of the complex regarding as a single unit:

$$f_{nH}^{(CX)} = f_{nH}^{(M)} \frac{1+4.75\times10^{-3}\varphi_{T3}}{1+\ 0.114\varphi_{T3}} \quad , \tag{3-17}$$

where superscript (S), (M) and (CX) denote satellite and master reactor, and the complex system, respectively. Evaluations of γ at the temperature making γ minimum are done and the results are listed in Table 2. We can see that the complex yields only 1.8 % greater γ than ^3He-Cat.D-G even after 100 years operation. We notice in eq.(3-15) that φ_{T3} will take approximately constant value of 0.9 after continuous operation during 40.8 years, which indicates ^3He-Cat.D-G system requires perpetual adjustment of external parameters because of slowly increasing φ_{T3}. In the case of the complex, however, steady state operation of the master at the fixed rating is warranted owing to complete separation of the master and the satellite. We believe the separation will bring forth further advantages that the cleaner satellite might be sited near urban areas [1] and also the cycles will be operated independently even if we are able to use ^3He from moon. In addition, it is considered that a D^3He reactor fed by ^3He from moon may also share the tritium reservoir although tritium inventory will increase to

some extent. Concurrently, we may say the complex is better system in comparison with ^3He-Cat.D-G's. Unfortunately, however, precise comparison between Cat.D system and the complex is not possible in straight forward manner at this time, because the complex requires huge amount of tritium storage for ^3He, so that for detailed comparison abundant knowledge about safety problems in tritium storage will be necessary.

3.3 Conceptual Design Parameters Of The Ignited Reactor

It is demonstrated that in preceding subsection Cat.D cycle or/and the complex will be the most promising candidate for fusion power plant applications. In this subsection we give examples of conceptual design parameters in order to figure out what will advanced fuel reactor look like.

Figure 7 shows a typical schematic drawing of a steady state reactor of FRC type, which is quite simple in construction as compared with an usual toroidal facility. Basically, an FRC reactor is composed of a single long solenoid ended by mirror coils attached to control the plasma radius [11] . We put energy convertors at both ends of the apparatus to collect energies from charged particles flowing out along the external field lines. It is noted that the convertor should have a function of particle sink like a divertor of a tokamak so that appropriate pumping system must always be instaled. Here, as in ref.[3] , we also assume plasma beam injection is possible across magnetic field [17] , because intensive diamagnetic current always forces the beam inside. And in the central section we put low energy particle injectors for particle supply

or fueling, and high energy injectors of CBI system for plasma heating up and trapped flux enhancement in order to bring the plasma into ignited state.

We notice advanced fuels do not require any tritium breeding system in the blanket, so that not only its construction becomes much simpler but also safety increases. Moreover, Ragheb and Salimi [18] demonstrated higher thermal efficiency is expected because of capability to afford higher temperature. Also, Dawson [19] pointed out that if the first wall is made of low Z materials such as *Be*, *B* or *C*, x-rays (bremsstrahlung) from the plasma core can be fairly transparent through the first wall as to give direct volume heating, which is favorable for heat removal.

Because our present task is in clarifying global pictures of advanced fuel reactors based on the self-consistent solutions presented so far, we conveniently give examples of designs giving 1000 MW power plant applications. In evaluating parameters we assume for simplicity that energy conversion efficiency η_{Elec} into electricity from neutrons, bremsstrahlung and plasma flows evenly takes the value of 40 %. We also assume limiting power density $q^{(w)}$ through/on the first wall is 4 MW/m^2 for both neutrons and bremsstrahlung, which is suggested by the STARFIRE study [20] and also by the anticipated unimportance of high energy particle hitting the wall because divertors are always built-in and the particle injection concept is free from neutrals. We choose σ_{ec}=0 because σ_{ec} has only insensitive effects unless σ_{ec} is very close to unity. Taking the thickness of the sum of the blanket and the radiation shield to be 1 m, we

have summarized the postulated basic parameters for the design in Table 3. Since the first wall radius R_W(=1.6 m) and R_s(=1.2 m) are given, the problem is to find out the length L of FRC capable to yield 1000 MW electricity. We know L can be estimated by the relation:

$$L = \frac{\hat{W}_{Fus}}{2\pi R_W q^{(w)}} \cdot \frac{\hat{W}_{n,brm}}{\hat{W}_{Fus}} \quad , \tag{3-18}$$

where for $\hat{W}_{n,brm}$ greater one out of $\hat{W}_n$ or $\hat{W}_{brm}$ is used.

Taking out the branch of the root belonging to lower burn fraction f_{B1}, we presented the evaluated results of L and other important parameters in Table 4. In estimating the mirror ratio R^* to control R_s [11], we use coil radius R_C rather than R_W because of the steady state assumption. Looking over Table 4, we find advanced fuel reactor can be very compact in size compared with a tokamak's [20]. In addition we are able to confirm following items.

(1) We observe τ_p is much greater than the relaxation times [21,22] of both 14 MeV protons ($\tau_r^{(p)}$) by D^3He reaction and 3.25 MeV α particles ($\tau_r^{(\alpha)}$) by DT reaction, so that a good foundation is rendered to the thermal plasma model.

(2) The burning FRC must be stable because $\bar{s}$ is estimated to be small enough.

(3) The smallness of the total required ion induced current $\hat{I}_+$ is confirmed, which even indicates the possibility, at least in the present estimation, that any special current driving system is not needed for the ignited plasma but the fueling system may be shared to generate sufficient

$\hat{I}_*$ as well.

(4) Tritium through put $\dot{M}_T$ is reduced by more than two orders of magnitude in advanced fuel cycles from the value of DT's.

(5) If tritium storage of 197 kg gives no serious effects on the safety problems, eqs.(3-15) and (3-16) show that after about 60 years operation of the master ^3He-Cat.D reactor we may have ^3He fuel enough to burn 140 MW D^3He reactor out of 1000 MW master reactor.

(6) Cat.D and ^3He-Cat.D reactor will be much compact in size compared with DT or D^3He system. This is because out put power density in the catalyzed system is equally shared among $\hat{W}_n$, $\hat{W}_{brm}$ and $\hat{W}_H$. It is noted that $\hat{W}_H$ is equal to the power carried by charged particles to the energy converters at the end of the apparatus.

Because we noticed $\bar{s}$ and $\hat{I}_*$ are dependent on the value of β_H rather sensitively, we will give primitive discussions on the validity of item (2) and (3) of above in the subsequent section.

4 DISCUSSIONS

Applicability to the present model is put into discussions. Because in the preceding section it is confirmed that τ_p is much greater than the relaxation times of both high energy protons and α particles produced by the fusion burn, we may say in a global sense the very basic assumption that thermal components dominate over the epithermal ones is satisfied.

However, problems exist in the sheath region near the plasma surface where electron density is low but plasma carries large amount of current because of sharp pressure gradient. High current density through a low density plasma may sometimes accompany such a high electron drift velocity v_e as to exceed over the thermal velocity. Since the boundary condition to the plasma is so chosen as to make v_e infinite at the separatrix, we conveniently compare v_e and v_{eth} on the surface located in the sheath where the field strength is reduced to $B_{ex}/2$. Then, we find $v_e \geqq v_{eth}$ is held for all the burn mode in Table 4. This indicates the basic assumption to the theory is violated in the thin region between the surface and the separatrix. Generalization of the theory to include epithermal particle's effects largely alters the equation sets, such that the pressure balance of the form eq.(2-1) and the Ohm's law of eq.(1-2) become no longer valid. Preliminary inspections to much general Ohm's law retaining epithermal terms show electrons are scattered away to diffuse out by the thermal force more effectively rather than the drag forces with ions in the velocity range $v_e \sim v_{eth}$ in contrast to the fact that the thermal force tends to improve the confinement under the thermal plasma model with $v_e \ll v_{eth}$. It is noted that the enhanced electron scattering induces larger thickness of the sheath. We also have several other mechanisms to increase the sheath thickness: neglected thermal conduction loss, especially that of electrons due to electron temperature gradient appearing near the separatrix [3], and some micro-instability which is liable to be excited at $v_e \geqq v_{eth}$. Unfortunately, since theoretical

investigations taking all these effects are in very infant stage, we are forced to choose phenomenological approach based on the simple thermal plasma model developed so far. From these reasons we introduce an empirical coefficient C_{emp} and write down the depth $d_{sh}^{(1/2)}$ of the surface having $B_{ex}/2$ in the following form after the modification of eq.(2-31):

$$d_{sh}^{(1/2)} = C_{emp} \frac{0.136}{\beta_H} R_s \qquad (4\text{-}1)$$

Equation (4-1) shows the sheath broadening is equivalently understood by the reduction of β_H by C_{emp} times or the enhancement of resisitivity η by C_{emp} times as may be suggested by the definitions of β_H and τ_d. Here, we notice in eq.(2-28) that β_H and $\bar{s}$ are inversely proportional to each other, so that the reduction of β_H leads to the increase of $\bar{s}$ and the plasma might become unstable to the internal tilting mode if $\bar{s}$ exceed over about 2 [5] . In this sense the increase of C_{emp} may make the plasma unstable so that the maximum value of C_{emp} is determined by the condition $\bar{s}$=2. In Table 5 approximate values of C_{emp} increasing those of $\bar{s}$ given in Table 4 to $\bar{s}$=2 are listed up. Because $\bar{s}$ is a function of temperature, we also evaluated permissible C_{emp} in case the 1000 MW reactor is operated at T=100 keV. Considering D^3He cycle of α_3=1.9 will not ignite at 100 keV, we refer the one of α_3=1.0 instead, and the results are given in Table 5.

Since introduction of C_{emp} is equivalent to the reduction β_H, the quantities related with the sheath may suffer considerable influence, although the global ones such as $\langle\beta\rangle$ or

τ_E is quite insensitive unless β_H goes down to as large as 3 or smaller. For reference, we show the case of C_{exp}=10 in Table 6 how $d_{sh}^{(c)}$, $\bar{s}$ and $\hat{I}_*$ increase from the ones in Table 4. Total current driving power $\hat{W}_{cd}$ listed in Table 6 is estimated using the same simple CBI model in ref. [3] . We find $\hat{I}_*$ is quite sensitive to the change of β_H. This is because $\hat{I}_*$ is determined by b' on the field null as suggested in eq.(2-27). Considering b' on the field null is affected by the source distribution rather sensitively, we may say $\hat{I}_*$ is highly model dependent quantity. In the case of a hollow distribution of σ_{ec} instead of a bell shaped one in Fig.2, we may expect much smaller $\hat{I}_*$ because the pressure gradient around the field null will be much smaller. Another factor making accurate estimation of $\hat{I}_*$ difficult exists in the importance of stress tensor $\bar{\bar{\pi}}$ around the field null where $\omega_i\tau_i \ll 1$ hold. Although ignorance of viscosity coefficient inhibits the accurate evaluation on the effect of $\bar{\bar{\pi}}$, tentative application of the Braginskii's [23] leads the conclusion that very small pressure gradient near the field null is supported by viscosity rather than magnetic pressure [4] . If so, the field gradient b' on the field null making $\omega_i\tau_i \sim 1$ on the separatrix is shown to be more than enough [4] . And we find $\omega_i\tau_i \sim 1$ on the separatrix gives the value of i equivalent to β_H=49 for Cat.D and ^3He-Cat.D cases in Table 4. Then, we easily have $\hat{I}_*$=180 A so that high energy CBI system requires 4.7 kW or the simpler single D^+ beam injection 3.9 kW. We would say that, because the CBI concept is introduced to simplify the analysis around field null, the simpler injection using only D^+ beam may be preferable in case stress tensors are taken into

account by proper method e.g. by numerical modeling.

Consequently, it may be inferred that upper limit of $\hat{I}_*$ or $\hat{W}_{cd}$ may be estimated by bell shaped distribution with $\sigma_{ec}=0$ because hollow distribution or the effect of $\bar{\bar{\pi}}$ always tends to decrease the required value of $\hat{I}_*$. However, we must note that $\hat{I}_*$ is the quantity uniquely determined by the boundary condition of the system as in eq.(2-37), so that the installation of the facility to control $\hat{I}_*$ for keeping required value is always necessary. This is true even in the ideal case having such a high β_H as $\hat{I}_*$ takes so small a value that sufficient amount may be generated by the plasma rotation, which may be induced by the balance between the injected angular momentum accompanied by fueling and the flow of the angular momentum near the fields null.

We have shown that quantities related with plasma profile in the core such as $\hat{I}_*$ involves rather model dependent nature, although the choice of any model gives quite insensitive effect to $\langle\beta\rangle$ and τ_E which are the most important to characterize the global plasma confinement property. We consider this comes from the fact that $\langle\beta\rangle$ and τ_E is determined exclusively by the sheath region because b_c becomes small enough if β_H is large. And we may say the perturbations given to the core must not be very significant. Then, we can easily imagine the case that the perturbation is given in the form of toroidal field. If toroidal field exists in the core, the configuration becomes that of spheromak. Consequently, it may be said that all the parameters other than $\hat{I}_*$ presented in Table 4 must be valid for a high beta toriodal system in general. However, we say FRC is

the simplest one of all.

At present, we have no accurate theoretical nor experimental information on the C_{exp} , because no *DD* nor *DT* ignition has ever been demonstrated so far. However, we may infer some preliminary values of C_{exp} using reversed field theta-pinch. Actually, self-consistent analysis of Hamada [9] shows that $Z_{eff}C_{exp} \leqq 9.3$ holds for variety of the recent FRC experiments. In addition, we demonstrated in ref. [3] that τ_p observed in FRX-C experiment at Los Alamos agrees quite nicely with our estimation by the present theory, although we know the comparison involves rather inadequate problem that the experiment is not in true steady state. Therefore, considering higher T_e tends to quench anomalies due to increased v_{eth} , we hopefully anticipate that $C_{exp} \leqq 70$ is satisfied. If so, we are able to construct an ideal *DD* ignited reactor.

5 CONCLUSIONS

A steady state self-consistent plasma modeling is demonstrated to be quite effective in solving the problems independently of any anomalous effects in case high power input $\hat{W}_H$ to the extent

$$\hat{W}_H \gg \frac{B_{ex}^2}{2\mu_0} \frac{\hat{V}_p}{\tau_d}$$

is ensured to keep the state $\langle\beta\rangle \sim 1$. It is pointed out that in such a state following peculiar characteristics and advantages

concerning the reactor aspect will come out.

(1) The field economy is maximized.

(2) The plasma gains homeostasis which stabilizes the thermal instability and enables the accurate estimation of τ_E.

(3) Current driving power and cyclotron loss are minimized.

(4) Macroscopic instabilities such as the internal tilting mode and the n=2 rotational mode are stabilized by kinetic effects accompanied by high $\langle\beta\rangle$.

In the reactor application point of view, achievement of ignited state is the most important item. And we have confirmed deuterium based fuel cycles actually ignite in the temperature ranges shown in Fig.3. Although pure *DD* cycle will not ignite, reinjection of fusion produced ^3He or/and tritium as a catalyzer will bring the system into ignition. In case storage of tritium for converting into ^3He will not cause serious environmental problems, the best cycle we have proposed is the complex composed of the main ^3He-Cat.D and satellite ^3He enriched D^3He cycle. If tritium storage is not allowed, we may utilize usual Cat.D cycle although 14 MeV neutron yield will increase by 35 % over the complex.

The notable advantages of the advanced fuel reactor of FRC type, which necessary satisfy $\langle\beta\rangle\sim 1$, are in simple linear construction in spite of toroidal field configuration, and in compactness in size; the plasma volume and the field strength of the present day large tokamak device such as JT-60 or others is found to be enough for 1000 MW power plant use. We say the simplicity is the privilege of FRC and compactness originates from the fact that catalyzed fuel cycles evenly share out the

fusion energy among neutrons, bremsstrahlung and charged particles' flow.

We conclude an advanced fuel reactor is safely granted with high priority to a candidate of the energy source resolving the eternal demands of mankind.

REFERENCES

[1] e.g. Miley, G.H.,Fusion Energy Conversion, American Nuclear Society (1976)

[2] e.g. Evans, K.Jr., Baker, C.C., Brooks, J.N., et al., ANL/FPP/TM-150

[3] Hirano, K., Submitted to Nuclear Fusion (IPPJ-801)

[4] Hirano, K., Nucl.Fusion 24 (1984) 1159

[5] Barns, D.C., Schwartzmeier, J.L., Seyler, C.E., Phys.Fluids. 29 (1986) 2616

[6] Berk, H.L., Sayer, J., Schnack, D.D., in Proc. of the US-JAPAN Joint Symposium on Compact Toruses and Energetic Particle Injection, PPl Princeton University, Princeton N.J. (1979) 122

[7] Ishimura, T., Private Communication (1986)

[8] Cordey, J.G., in Proc. of the Course on the Theory of Magnetically Confined Plasma, Varenna, (1977) lecture 2

[9] Hamada. S., Nucl.Fusion 26 (1986) 729

[10] Barns, D.C., Seyler, C.E., Andeson, V.D., in Proc. of the US-JAPAN Joint Symposium on Compact Toruses and Energetic Particle Injection, PPL Princeton University, Princeton N.J. (1979) 457

[11] Suzuki, K., Hamada, S., J. Phys. Soc. Japan 53 (1984) 16

[12] Dawson, J.M., P. DG.-273 UCLA (1975)

[13] Maxson, S., Phys. Rev. A5 (1972) 1630

[14] McNally, J.R.,Jr., Roth, K.E., Snarp, R.D., ORNL/TM-6914 (1979)

[15] Wittenberg, L.J., Santarius, J.F., Kulchinski, G.L., Fusion Technology 10 (1986) 167

[16] Gross, R.A., Fusion Energy,John Wily & Sons, New York (1984)

[17] Rose, J.D., Clark, M., Jr.,Plasma and Controlled Fusion, The M.I.T. press and John Wily & Sons, New York (1961)

[18] Ragheb, M.M.H., Salimi, E., Nuclear Technology/Fusion 2 (1982) 55

[19] Dawson, J.M., Fusion 1 part B (1981)453

[20] Baker, C.C., Carlson, G.A., Krakowski, R.A., Nuclear Technology/Fusion 1 (1981) 5

[21] Siuvukin, D.V., Review of Plasma Physics 4, Consultant Bureau, New York (1966)

[22] Stix, H.S., Plasma Phys. 14 (1972) 367

[23] Braginskii, S.I., Review of Plasma Physics 1 Consultant Bureau, New York (1965)

FIGURE CAPTIONS

Fig.1. An elongated 1-D cylindrical FRC plasma model.

Fig.2. Assumed source distribution.

Fig.3. Temperature ranges that *DT* and D^3He cycles are ignited as a function of relative feeding rate of *T* and ^3He to *D*'s. Inside the contoures the plasma is ignited.

Fig.4. Bifurcated Lawson parameters for *DT*, D^3He, Cat.D and ^3He-Cat.D cycles as a function of plasma temperature.

Fig.5. Temperature dependences of various parameters to the ignited FRC reactors of 50-50 *DT* and ^3He highly enriched D^3He cycles having the reference values of $n_D=1\times10^{20}$ m^{-3} and $R_s=1$ m.

Fig.6. A block diagram for general catalyzed *DD* system with D^3He satellite and reservoir to convert *T* into ^3He to be burnt in the satellite.

Fig.7. A schematic drawing of an elongated FRC reactor.

TABLE CAPTIONS

Table 1. .Open and closure of the valves for proposed catalyzed *DD* cycles.

Table 2. Relative 14 MeV neutron flux γ of advanced cycles to 50-50 *DT*'s.

Table 3. Postulated basic parameters of an FRC reactor for a power plant applications.

Table 4. Evaluated parameters from the postulated ones.

Table 5. Empirical coefficient C_{emp} making $\bar{s}=2$.

Table 6. Expected plasma parameters at C_{exp}=10 .

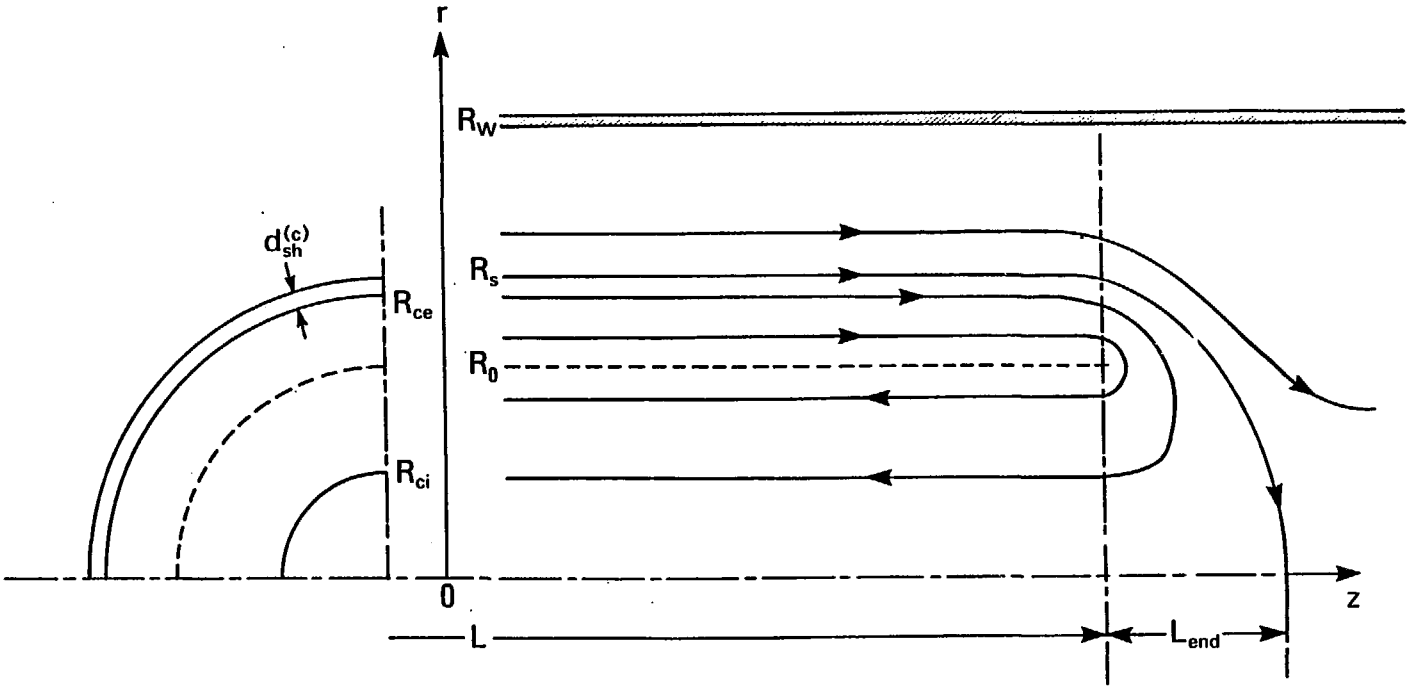

Fig.1

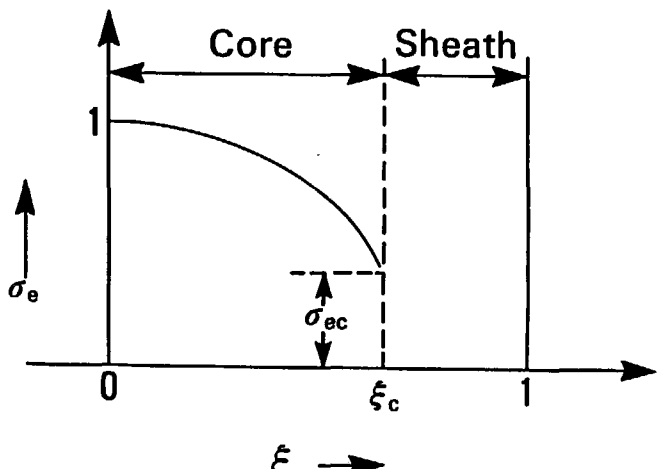

Fig.2

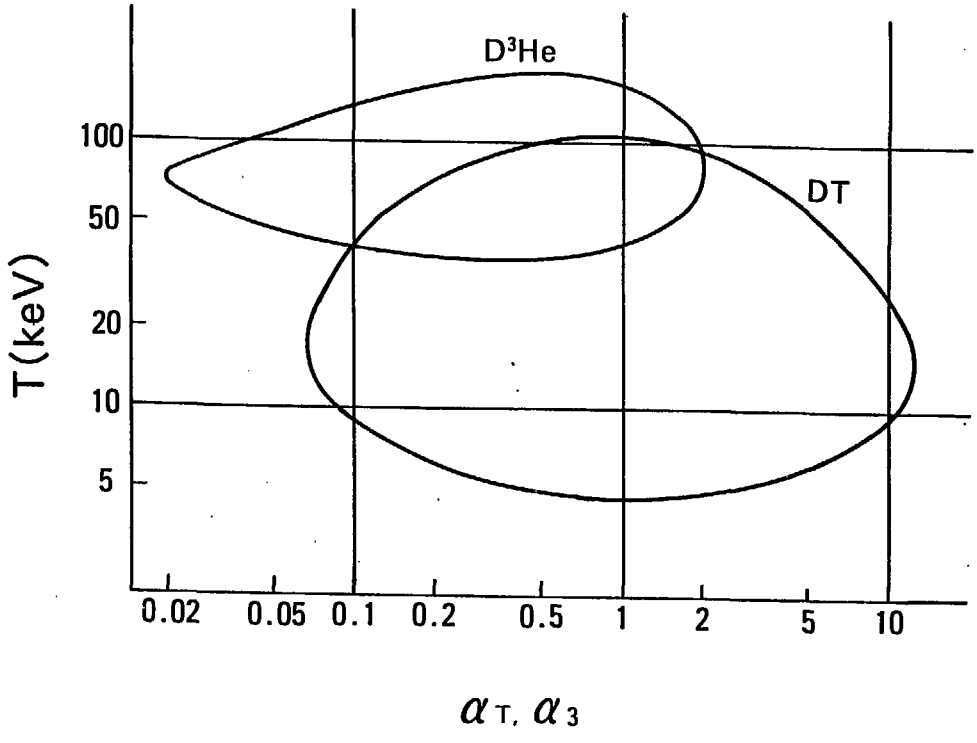

Fig.3

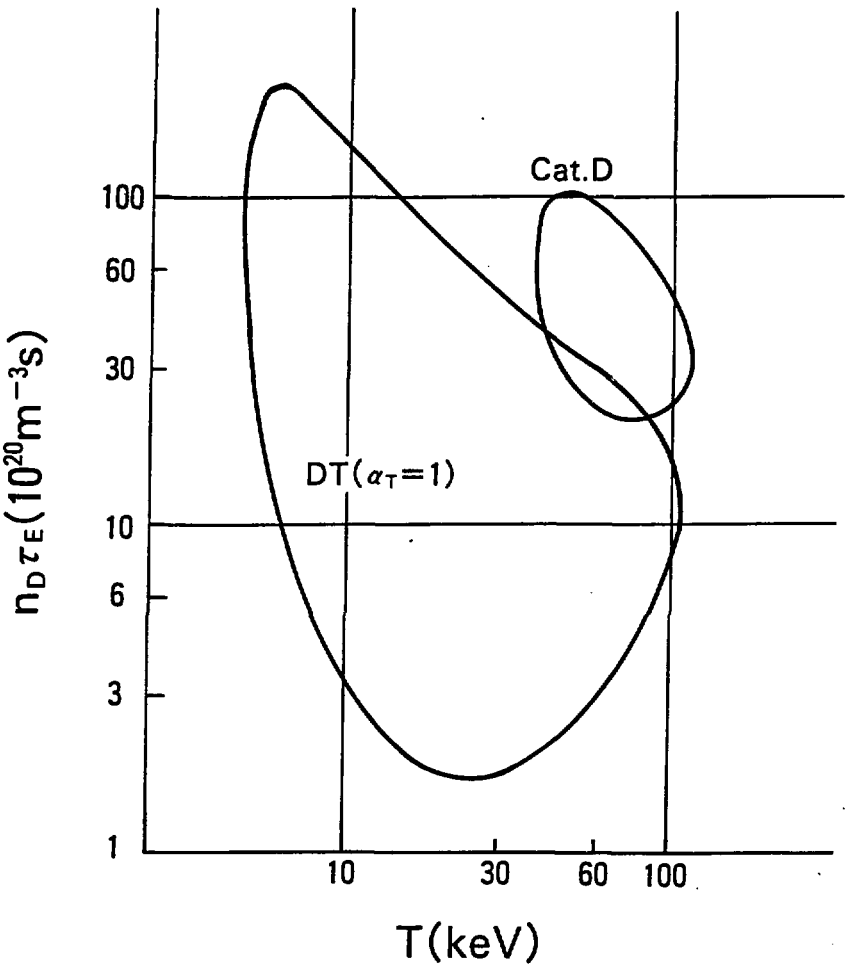
Cat.D
DT(α_T=1)
100
60
30
10
6
3
1
10
30
60
100
T(keV)
$n_D\tau_E(10^{20}m^{-3}s)$

Fig.4-a

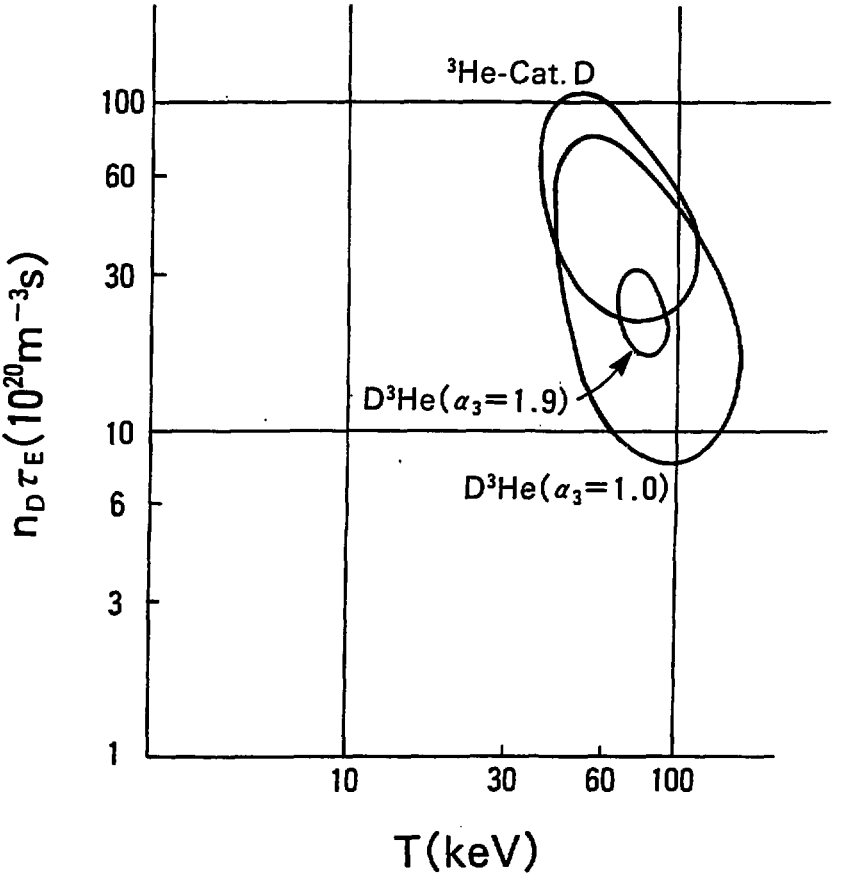
^{3}He-Cat. D
100
60
30
10
6
3
1
$n_D\tau_E(10^{20}m^{-3}s)$
D^{3}He(α_3=1.9)
D^{3}He(α_3=1.0)
10
30
60
100
T(keV)

Fig.4-b

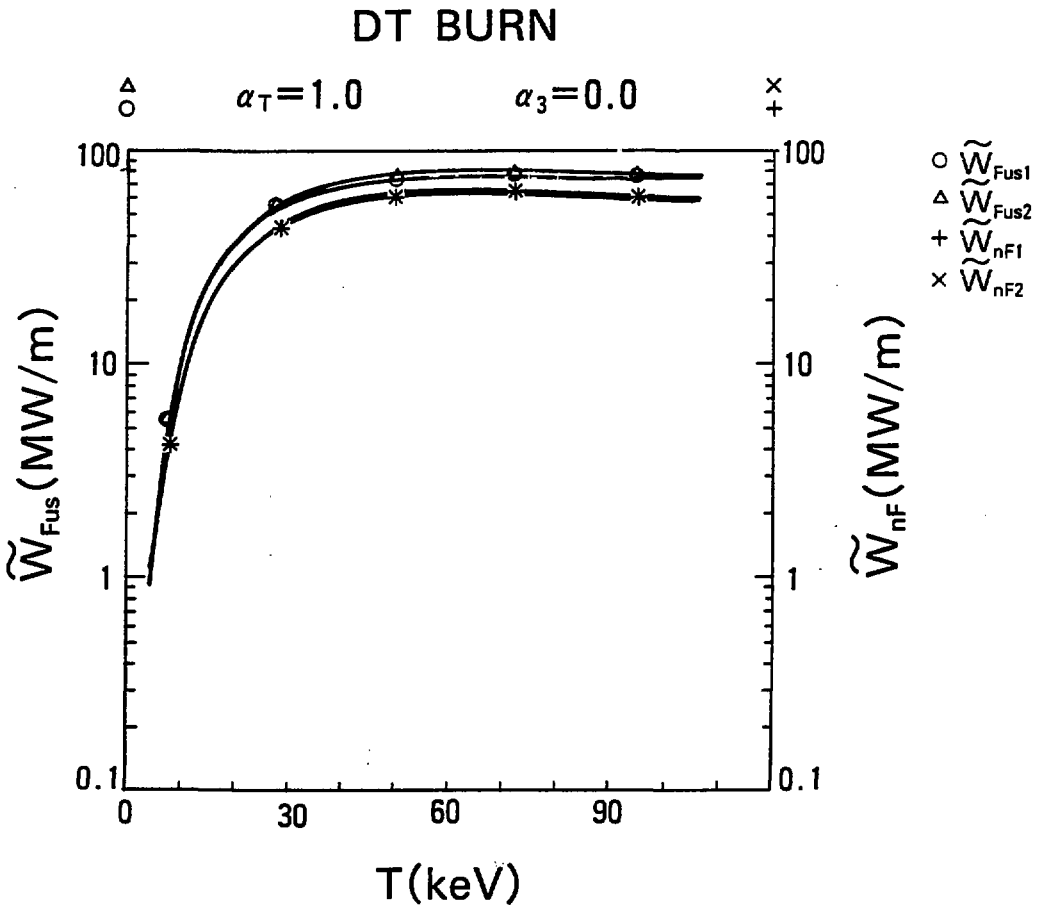
DT BURN
△ ○ α_T=1.0 α_3=0.0 × +
100
10
1
0.1
0
30
60
90
T(keV)
$\tilde{W}_{Fus}$(MW/m)
$\tilde{W}_{nF}$(MW/m)
○ $\tilde{W}_{Fus1}$
△ $\tilde{W}_{Fus2}$
+ $\tilde{W}_{nF1}$
× $\tilde{W}_{nF2}$

Fig.5-a

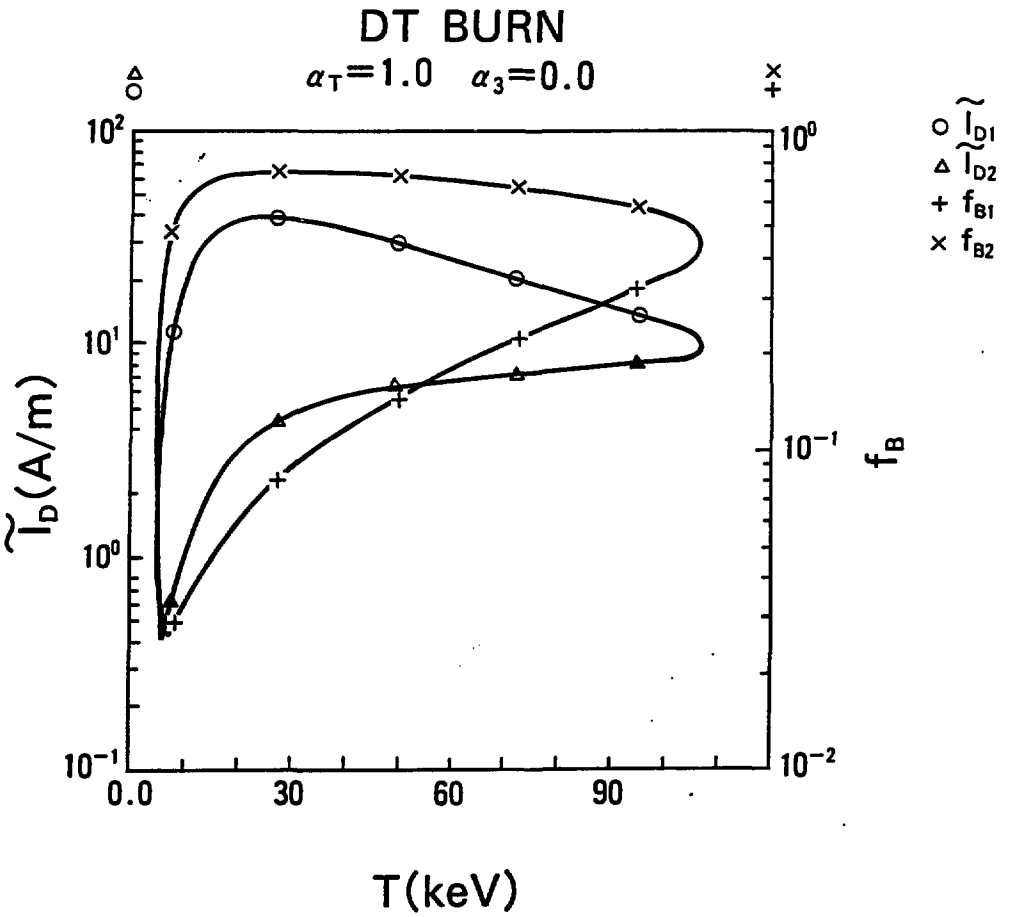
DT BURN
α_T=1.0 α_3=0.0
$\tilde{I}_{D1}$
$\tilde{I}_{D2}$
f_{B1}
f_{B2}
$\tilde{I}_D$(A/m)
f_B
T(keV)
10^2
10^1
10^0
10^{-1}
10^0
10^{-1}
10^{-2}
0.0
30
60
90

Fig.5-b

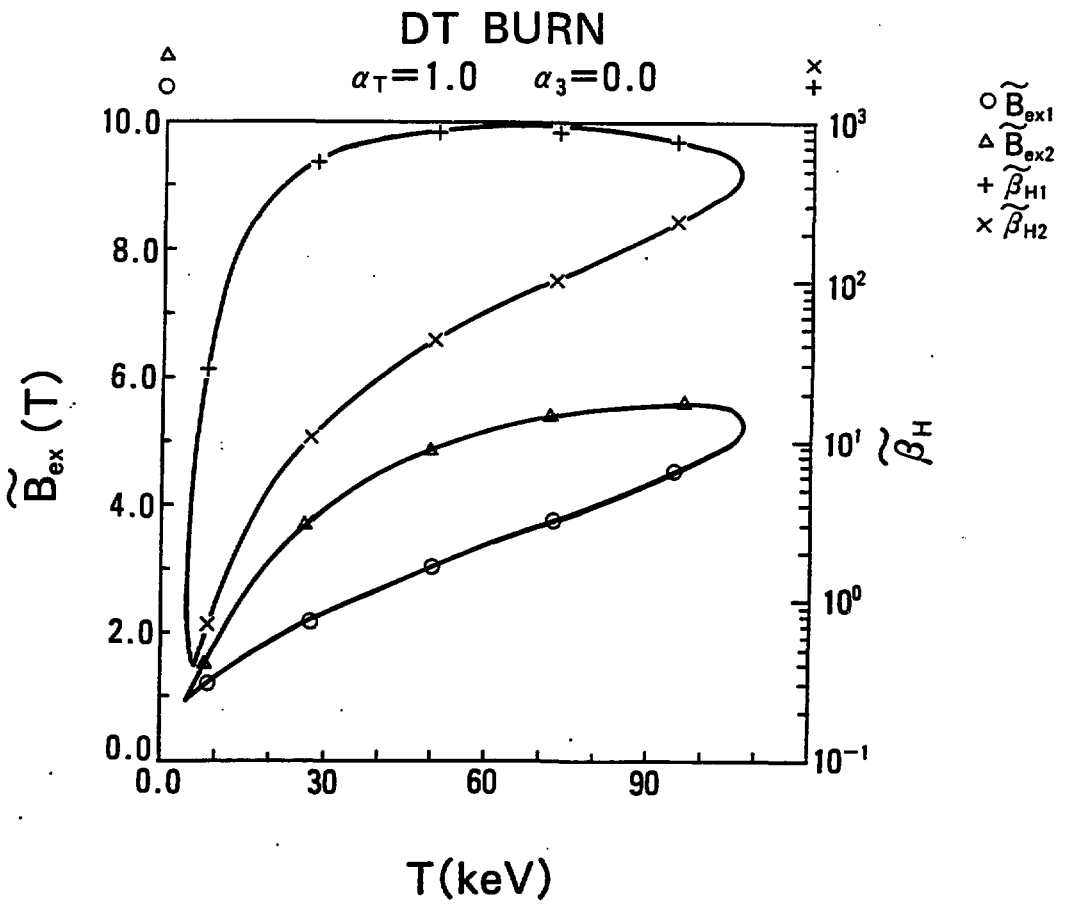
DT BURN
α_T=1.0 α_3=0.0
$\tilde{B}_{ex}$ (T)
$\tilde{\beta}_H$
T(keV)
$\circ\ \tilde{B}_{ex1}$
$\triangle\ \tilde{B}_{ex2}$
$+\ \tilde{\beta}_{H1}$
$\times\ \tilde{\beta}_{H2}$

Fig.5-c

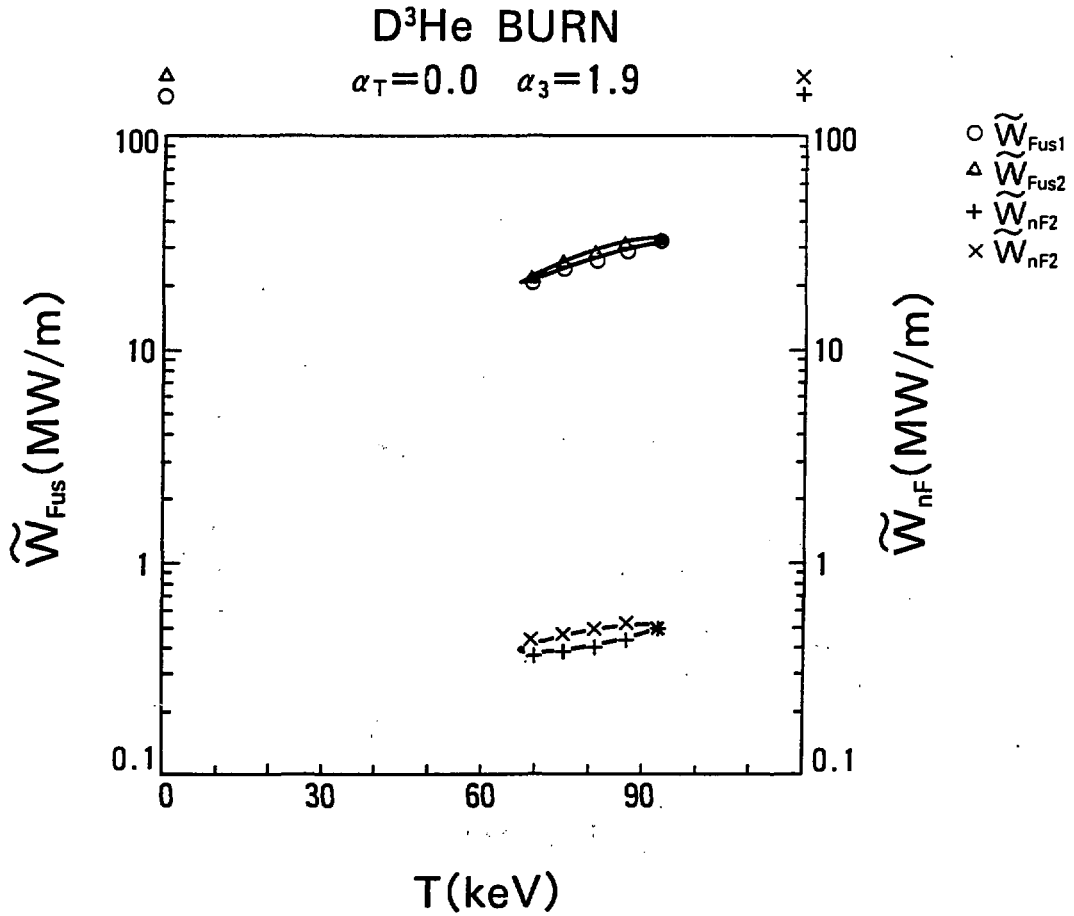
D³He BURN
α_T=0.0 α_3=1.9
$\widetilde{W}_{Fus1}$
$\widetilde{W}_{Fus2}$
$\widetilde{W}_{nF2}$
$\widetilde{W}_{nF2}$
$\widetilde{W}_{Fus}$(MW/m)
$\widetilde{W}_{nF}$(MW/m)
100
10
1
0.1
0
30
60
90
T(keV)

Fig.5-d

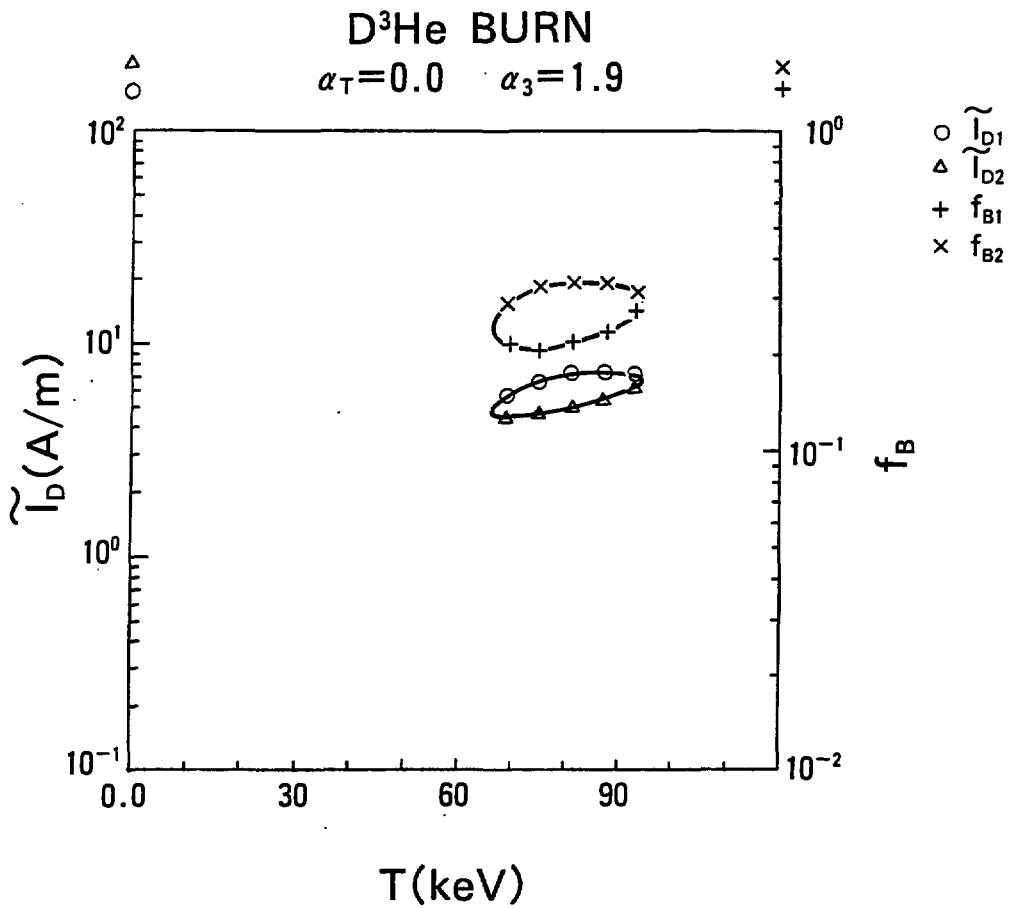
D³He BURN
αT=0.0 α3=1.9
10²
10¹
10⁰
10⁻¹
0.0
30
60
90
T(keV)
Ĩ_D(A/m)
10⁰
10⁻¹
10⁻²
f_B
Ĩ_D1
Ĩ_D2
f_B1
f_B2

Fig.5-e

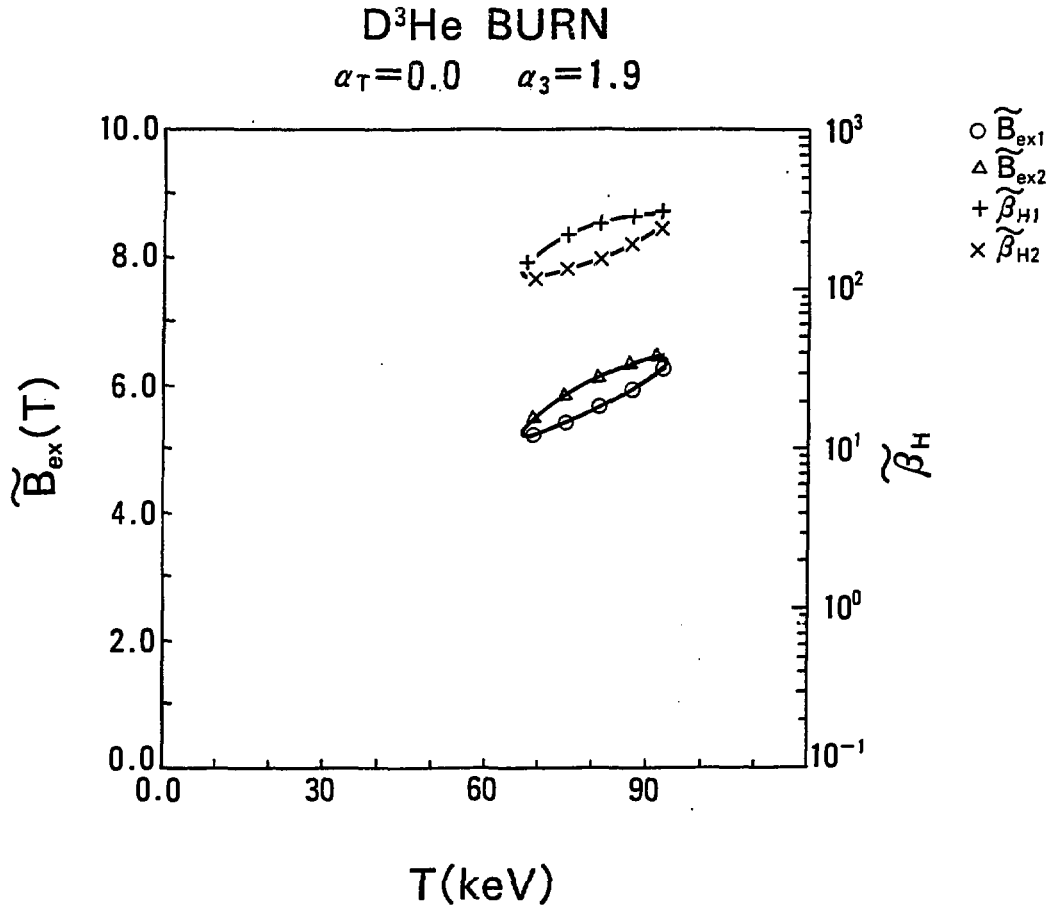
D³He BURN
α_T=0.0 α_3=1.9
$\tilde{B}_{ex}$(T)
$\tilde{\beta}_H$
T(keV)
10.0
8.0
6.0
4.0
2.0
0.0
0.0
30
60
90
10^3
10^2
10^1
10^0
10^{-1}
○ $\tilde{B}_{ex1}$
△ $\tilde{B}_{ex2}$
+ $\tilde{\beta}_{H1}$
× $\tilde{\beta}_{H2}$

Fig.5-f

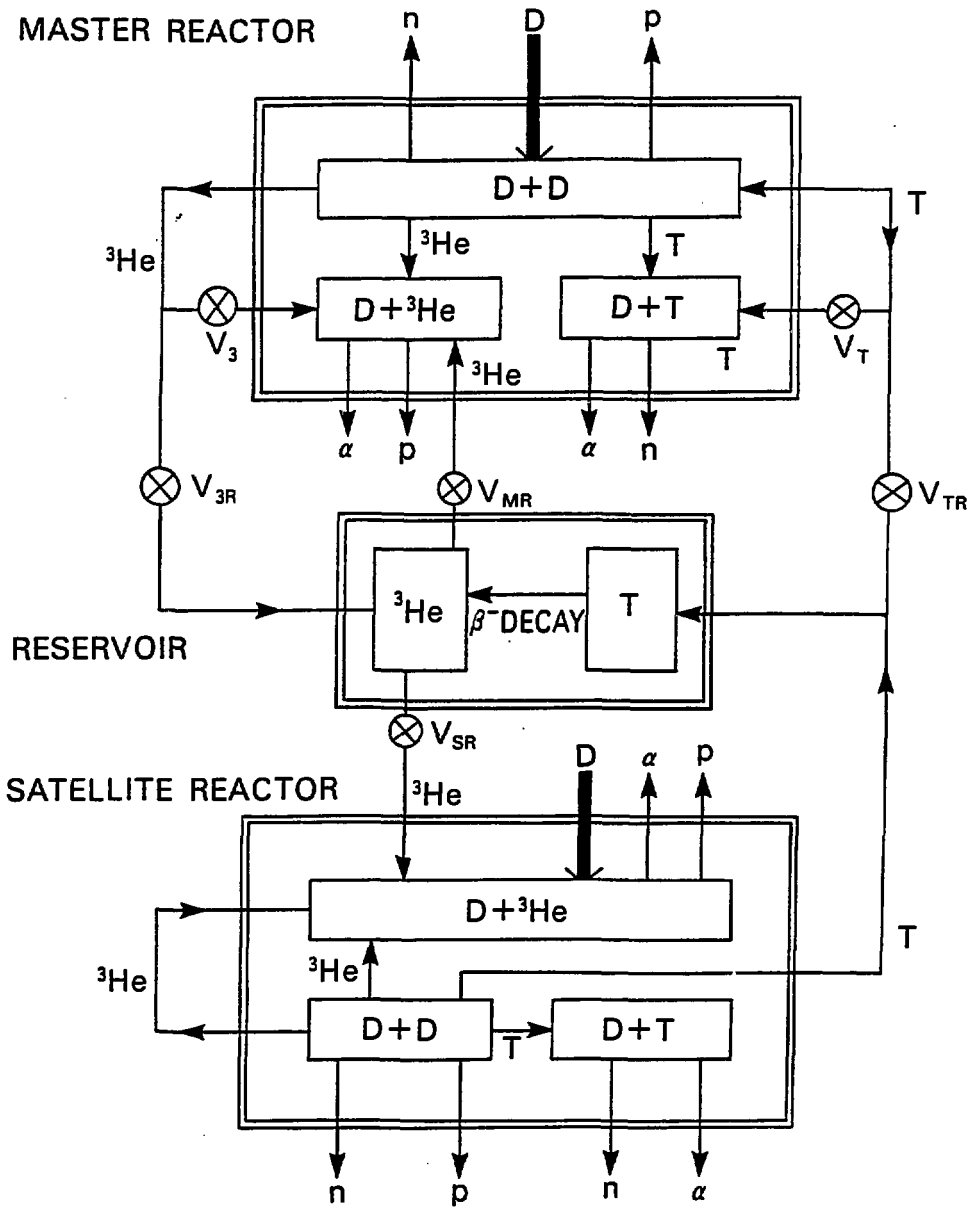
MASTER REACTOR
n
D
p
D+D
T
³He
³He
T
D+³He
D+T
V₃
V_T
T
³He
α
p
α
n
V_3R
V_MR
V_TR
³He
β⁻DECAY
T
RESERVOIR
V_SR
D
α
p
SATELLITE REACTOR
³He
D+³He
T
³He
³He
D+D
T
D+T
n
p
n
α

Fig.6

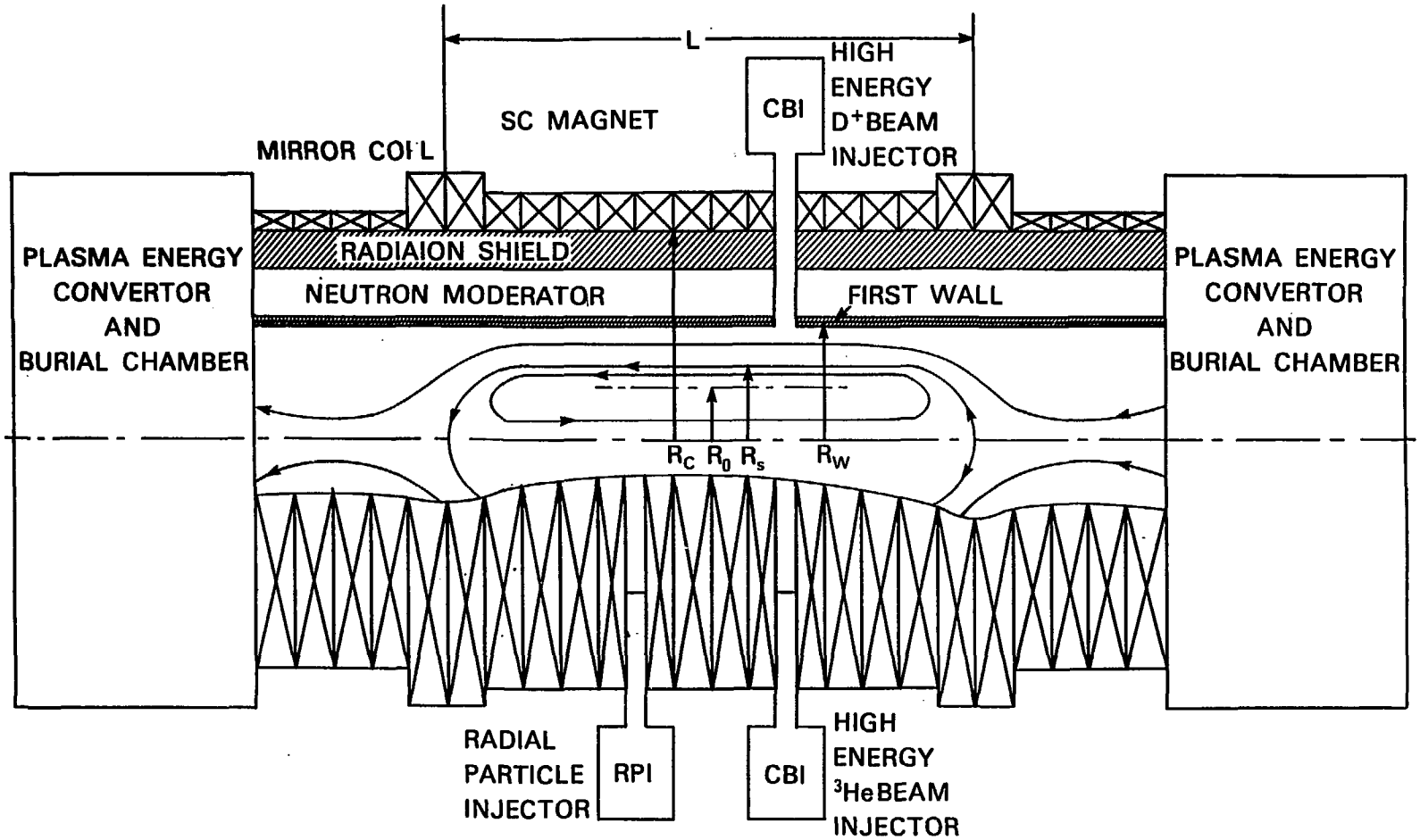
L
SC MAGNET
CBI
HIGH
ENERGY
D+BEAM
INJECTOR
MIRROR COIL
PLASMA ENERGY
CONVERTOR
AND
BURIAL CHAMBER
RADIAION SHIELD
NEUTRON MODERATOR
FIRST WALL
PLASMA ENERGY
CONVERTOR
AND
BURIAL CHAMBER
R_C R_0 R_s R_W
RADIAL
PARTICLE
INJECTOR
RPI
CBI
HIGH
ENERGY
^{3}HeBEAM
INJECTOR

Fig 7

TABLE 1

	V_T	V_3	V_{TR}	V_{3R}	V_{HR}	V_{SR}
Cat.D	O	O	C	C	C	C
^{3}He-Cat.D	C	O	O	C	C	O
^{3}He-Cat.D-G	C	O	O	C	O	C

TABLE 2

TYPE OF ADVANCED FUEL CYCLES		γ (percent)
D^3He:	α_3 = 1.9	1.22
	α_3 = 1	2.08
	α_3 = 0.5	4.77
Cat.D		36.4
^{3}He-Cat.D-G:	t = 0 (Y)	29.9
	t = 10 (Y)	27.9
	t = 30 (Y)	26.0
	t = 100 (Y)	25.2
COMPLEX:	t = 0 (Y)	29.9
	t = 10 (Y)	28.5
	t = 30 (Y)	27.5
	t = 100 (Y)	27.0

N.B.: 1) f_{nH} is measured at the temperature making f_{nH} minimum, 2) $f_{nH}^{(DT)} = 3.55\times10^{20}$ neutrons/GJ.

TABLE 3

$\hat{W}_{Elec}$	(MW)	1000
R_s	(m)	1.2
R_w	(m)	1.6
R_C	(m)	2.6
η_{Elec}		0.4
$q_{brm}^{(w)}$	(MW m^{-2})	4
$q_n^{(w)}$	(MW m^{-2})	4
σ_{ec}		0

TABLE 4-A

	DT	Cat.D	^3He-Cat.D	D^3He
L (m)	49.7	22.3	23.0	36.9
T (eV)	20	45	45	73
n_D (10^{20} m^{-3})	0.96	8.75	9.01	1.43
n_e (10^{20} m^{-3})	2.04	12.1	12.5	8.70
B_{ex} (T)	1.8	6.4	6.5	6.4
R^*	1.27	1.27	1.27	1.27
$\hat{I}_D$ (kA)	2.4	2.8	3.0	0.68
$\hat{I}_T$ (kA)	2.4	0.012	0	0
$\hat{I}_3$ (kA)	0	0.28	0.27	1.3
$\hat{W}_n$ (MW)	1980	890	823	41
$\hat{W}_{brm}$ (MW)	26	842	922	1477
$\hat{W}_H$ (MW)	480	747	792	970
$\hat{\Gamma}_{nH}$ (10^{20} s^{-1})	8.94	3.27	2.90	0.125
$\hat{\Gamma}_{ntot}$ (10^{20} s^{-1})	8.96	7.16	7.20	0.451
$\dot{M}_T$ ($g(day)^{-1}$)	6490	32.5	27.4	1.94
$M_{t\infty}^{(R)}$ (kg)			197	

N.B. : $\hat{\Gamma}_n$ denotes neutron yield in the reactor with suffix H being 14 MeV component, $\dot{M}_T$ is tritium through put and $M_{t\infty}^{(R)}$ final amount of tritium storage in the reservoir.

TABLE 4-B

	DT	Cat.D	^3He-Cat.D	D^3He
β_H	470	370	370	420
$n_0\tau_E$ (10^{20} sm^{-3})	1.7	32	34	19
τ_p (s)	3.0	6.1	6.3	22.3
$\tau_r^{(p)}$ (s)	0.85	0.38	0.37	0.93
$\tau_r^{(\alpha)}$ (s)	0.26	0.076	0.074	0.13
$\overline{s}$	0.043	0.13	0.13	0.089
Z_{eff}	1.06	1.24	1.24	1.79
f_B (%)	5.9	8.2	8.2	21
$d_{sh}^{(c)}$ (cm)	0.29	0.35	0.35	0.32
R_{ci} (cm)	8.4	9.2	9.2	8.7
B_c (T)	0.077	0.31	0.31	0.29
$\hat{I}_+$ (A) ($10^{-N}\rightarrow(N)$)	1.0(51)	7.1(39)	7.4(39)	7.6(45)

TABLE 5

	DT	Cat.D	^3He-Cat.D	D^3He
C_{esp}	100	20	20	30
T (keV) (α_3)	20	45	45	73 (1.9)
C_{esp}		70	70	120
T (keV) (α_3)		100	100	100 (1.0)

TABLE 6

	DT	Cat.D	^3He-Cat.D	D^3He
β_H	47	37	37	42
$d_{sh}^{(c)}$ (cm)	1.6	1.9	1.9	1.8
$\bar{s}$	0.36	1.1	1.1	0.76
$\hat{I}_+$ (kA)	0.20	5.4	5.7	2.2
$\hat{W}_{cd}$ (kW)	1.8	140	140	38